AD-A191 858 IMPACT DAMAGE TOLERANCE OF CARBON FIBRE AND HYBRID LAMINATES(U) ROYAL AIRCRAFT ESTABLISHMENT FARNBOROUGH (ENGLAND) G DOREY ET AL. OCT 87 RAE-TR-87057 1/1

UNCLASSIFIED DRIC-BR-104549 F/G 11/4 NL

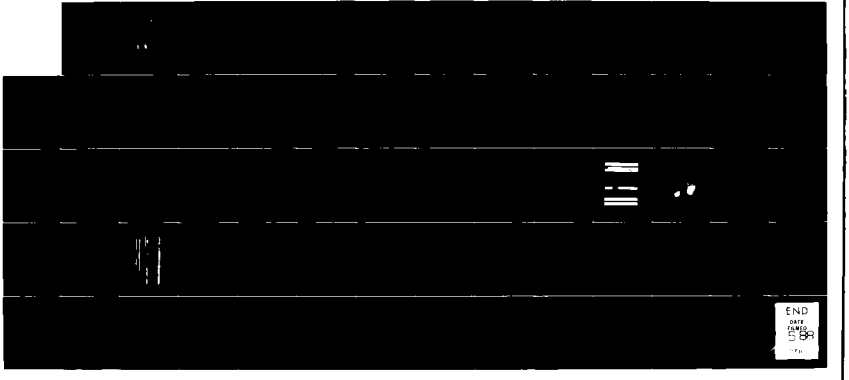

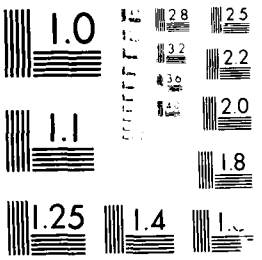
1.0
1.1
1.25
1.4
2.8
3.2
3.6
4.0
2.5
2.2
2.0
1.8

ROYAL AIRCRAFT ESTABLISHMENT

Technical Report 87057

October 1987

GARTEUR TP-037

IMPACT DAMAGE TOLERANCE OF CARBON FIBRE AND HYBRID LAMINATES

by

G. Dorey
P. Sigéty
K. Stellbrink
W.G.J. 't Hart

Procurement Executive, Ministry of Defence
Farnborough, Hants

ROYAL AIRCRAFT ESTABLISHMENT

Procurement Executive, Ministry of Defence
Farnborough, Hants

REPORT DOCUMENTATION PAGE

Overall security classification of this page

UNCLASSIFIED

As far as possible this page should contain only unclassified information. If it is necessary to enter classified information, the box above must be marked to indicate the classification, e.g. Restricted, Confidential or Secret.

1. DRIC Reference (to be added by DRIC)	2. Originator's Reference	3. Agency Reference	4. Report Security Classification/Marking
	RAE TR 87057		UNCLASSIFIED

5. DRIC Code for Originator	6. Originator (Corporate Author) Name and Location
7673000W	Royal Aircraft Establishment, Farnborough, Hants, UK
5a. Sponsoring Agency's Code	6a. Sponsoring Agency (Contract Authority) Name and Location

7. Title: Impact damage tolerance of carbon fibre and hybrid laminates

7a. (For Translations) Title in Foreign Language

7b. (For Conference Papers) Title, Place and Date of Conference

8. Author 1. Surname, Initials	9a. Author 2	9b. Authors 3, 4	10. Date	Pages	Refs.
Dorey, G.	Sigéty, P.	*et al*	October 1987	66	5

11. Contract Number	12. Period	13. Project	14. Other Reference Nos.
			Mat/Str 206

15. Distribution statement

(a) Controlled by –

(b) Special limitations (if any)

If it is intended that a copy of this document shall be released overseas refer to RAE Leaflet No.3 to Supplement 6 of MOD Manual 4.

16. Descriptors (Keywords) (Descriptors marked * are selected from TEST)

17. Abstract

This was the second phase of a collaborative research programme on impact damage tolerance of composite materials, carried out at four European aerospace research establishments under the auspices of GARTEUR (Action Group SM/AG01). The first phase had been a round robin that established that the four laboratories could produce similar results on a common carbon fibre laminate, showing that barely visible impact damage (BVID) significantly reduced the static strength but had little effect on the fatigue strength at 10^6 cycles of fully reversed axial loading. The second phase tended to confirm the results of phase one over a wider range of materials and test parameters. Studies were made of the damage produced on impact and damage growth under fatigue loading. Improvements in performance were achieved by the use of surface plies of various fabrics.

F5910/1

RAE Form A143 (revised October 1980)

N A T I O N A L A E R O S P A C E L A B O R A T O R Y

Technical Report [illegible]

GARTEUR TP-[illegible]

Received for printing [illegible]

COMPACT DAMAGE TOLERANCE OF CARBON FIBRE AND HYBRID LAMINATES

by

C. Bathy

[illegible]*

[illegible]**

W. G. [illegible]***

SUMMARY

This was the second phase of a collaborative research programme on impact damage tolerance in composite materials, carried out at four European aerospace research establishments under the auspices of GARTEUR (Action Group AM Aero1). The first phase (Bathy, Bathy and Harris) established that the four laboratories could produce similar results on a common carbon fibre laminate, showing that impact damage (BVID) significantly reduced the static strength but had little effect on the fatigue strength at low cycles of fully reversed axial loading. The second phase tended to confirm the results of phase one over a wider range of materials and test parameters. Studies were made of the damage threshold for impact and damage growth under fatigue loading. Improvements in performance were achieved by the use of surface plies of various fabrics.

Departmental Reference: Materials Structures 20b

[illegible]

* at ONERA Chatillon France

** at DFVLR Stuttgart Germany

*** at NLR Amsterdam Holland

LIST OF CONTENTS

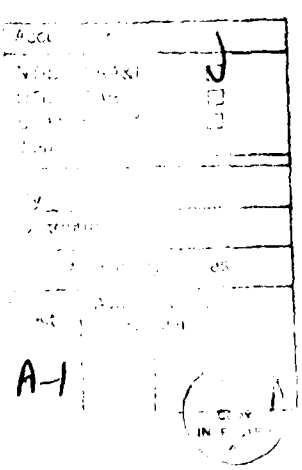

1 INTRODUCTION

Carbon fibre reinforced plastics (CFRP) are strong, stiff and light, and are therefore being used increasingly in aircraft structures to save mass and to improve performance. However, the full potential of these materials cannot be realised because they are susceptible to impact damage. In general, broken fibres significantly reduce the tensile strengths of CFRP laminates and delaminations reduce the compressive strengths. For penetrated laminates the damage is clearly visible and the reduction in strength is similar to that for machined holes. But for low energy impact, produced by dropped tools, runway stones or other causes, the barely visible impact damage (BVID) can significantly reduce the compressive strength and cannot be seen readily on inspection.

The GARTEUR action group SM/AG01, comprising DFVLR of Germany, NLR of Holland, ONERA of France and RAE of England, was formed to investigate the impact damage tolerance of CFRP laminates, to characterise and improve their performance. In phase 1 of the work, the group focussed on BVID and on the possibility of damage growth from BVID under fatigue loading, using common materials and test parameters to confirm that the four laboratories produced similar results[1]. In phase two, the four laboratories studied a wider range of materials and test parameters, making a more detailed study of damage growth and investigating potential improvements in damage tolerance by using hybrid laminates[2-5].

This Report summarises the results from the four laboratories for the work carried under phase two.

2 PHASE ONE

A common batch of unidirectional fibre/epoxy (T300/914C) prepreg was obtained from Ciba-Geigy (UK) Ltd, and moulded into laminates with a $[0,90,0,\pm45,0]_s$ lay-up at each of the four laboratories. Preliminary impact tests with well specified drop-weight facilities established a BVID threshold of 3 J, which had little effect on the residual tensile strength but which significantly reduced the residual compressive strength. Specimens, with and without this BVID, were tested under fully reversed axial fatigue loading ($R = -1$), using specified anti-buckling guides. The fatigue behaviour was dominated by the compressive loading and the S-N curves were similar for the four laboratories. There was a marked reduction in fatigue strength at short lifetimes, but the S-N curve for the damaged specimens was very flat and at 10^6 cycles there was little difference between the fatigue strengths for the damaged and undamaged specimens.

These results were encouraging for the application of CFRP in aircraft structures but more work was needed, over a wider range of variables, before more general conclusions on the impact damage tolerance of carbon fibre composites could be drawn. This was to be the aim of phase two.

3 PHASE TWO

As a result of phase 1, members of the group from the four laboratories drew up the proposed programme outlined in Table 1. Modifications, both additions and deletions, were made as the work proceeded, but it embodied the principles outlined (see tables 2, 3 and 4). A common core of the programme was the T300/914 CFRP material with the common $[(+45)_2 0_4]_S$ lay-up. RAE, NLR and DFVLR investigated possible improvements by using woven fabrics or hybrids. ONERA included T300/5208 and DFVLR included T300/Code 69 as matrix variations. NLR included ARALL to compare its performance with that of CFRP laminates. RAE, ONERA and DFVLR studied different lay-up effects. ONERA, and DFVLR varied the conditions of impact. ONERA and RAE included machined holes for comparison. RAE and NLR studied residual static strengths. ONERA, NLR and DFVLR measured residual fatigue properties at R = -1 and ONERA did additional testing at R = 10. All four laboratories used ultrasonic C-scan facilities to measure impact damage, ONERA and NLR monitored damage growth, and NLR prepared some polished cross-sections through damaged regions.

4 MATERIALS

The four laboratories had a common batch of unidirectional (UD) carbon fibre/epoxy prepreg material from Ciba-Geigy Ltd, designated Fibredux 914C-TS-5-34%, comprising T300 carbon fibres in BSL 914C resin, in the form of warp sheet 300 mm wide with a moulded thickness of 0.125 mm and a nominal fibre volume fraction of 60%.

In addition, other preimpregnated materials were obtained to study possible improvements in impact damage tolerance by mixing materials to form hybrids. DFVLR used UD E-glass fibres in 914 epoxy (914C-E-S) and a woven T300 carbon fibre fabric in 914 epoxy (914-C-814NT). NLR and RAE used common batches of a woven carbon fibre fabric in 914 epoxy (914C-Brochier G-807-34%), a woven aramid fibre fabric in 914 epoxy (914C-Kevlar type 285-37%) and a glass fibre fabric in 914 epoxy (914C-G7781-25%). ONERA had a batch of UD T300/5208 carbon fibre epoxy from Nimco and DFVLR had a batch of UD T300/Code 69 carbon fibre/epoxy from Fothergill and Harvey Ltd, to compare with the T300/914. The fabrics moulded to a thickness approximately 0.25 mm, twice that of the UD materials, and had a

slightly lower fibre volume fraction of about 55%. In hybrids, where fabrics replaced UD plies, one layer of fabric replaced two UD plies, either (0,90) or (±45).

NLR included an ARALL (aramid reinforced aluminium alloy) designed on the basis of equal weight/surface area compared with the 'protected' base laminates, resulting in a built-up laminate consisting of three 0.35mm layers of 7075-T6 aluminium alloy sheet and two intermediate 0.2mm layers of UD aramid reinforced adhesive.

The materials were laid up in the stacking sequences shown in Tables 1 to 4 and moulded in autoclaves in the four countries to the recommended cure schedules.

Some basic laminate properties are given in Tables 5-7 and in Figs 1 and 2. Others may be read from residual strength curves for zero impact energy or from S-N fatigue curves at one cycle.

The base laminates, $[(\pm 45)_2 0_4]_{3S}$, with 50% 0 deg plies, had tensile strengths between 850 and 975 MPa. With more dispersed 0 deg plies (Fig 1, lay-ups B and C) the tensile strengths were slightly lower at under 800 MPa. Replacing the ±45 deg carbon fibre plies with carbon fibre, aramid fibre or glass fibre fabrics gave increased tensile strengths, especially with the more dispersed 0 deg plies. This indicates that shear cracks parallel to the fibres in the 45 deg carbon fibre plies applied stress concentrations to the 0 deg load carrying plies. This would be less apparent in the base laminate where the 0 deg plies were in a block of eight plies, and where the 45 deg plies were fabric where shear cracks would be shorter and more dispersed.

The 10mm centre notches (Fig 1) reduced the tensile strengths to approximately half those of the unnotched laminates, with the exception of one specimen of lay-up A in which extensive delamination effectively decoupled the 0 deg and ±45 deg plies. However the failure loads indicated toughnesses of 40-50 MPa$\sqrt{m}$, which compares favourably with thick sections of other tough structural materials, but is considerably less than toughness values of thin sheet aluminium alloys. Again the detrimental effects of 45 shear cracks in lay-ups B and C can be seen clearly. Fig 3 shows ultrasonic C-scans of notched tensile specimens after testing. The delamination in lay-up A shows clearly and this gave good notched strength. The 45 deg cracking is evident in lay-ups B and C, resulting in lower failure stresses. The use of 45 fabrics in lay-ups D to I clearly reduced the incidence of 45 deg cracking and allowed a certain amount of 0 deg cracking which is most effective in reducing the stress concentration associated with the notch.

The ARALL (Table 5) had a tensile strength of 845 MPa, similar to those of the CFRP laminates, but with a failure strain over twice as great, indicating significant plastic strain.

Compressive strengths were lower, between 600 and 700 MPa, as in this case the laminates with the more dispersed 0 deg plies gave the highest values (Fig 2, lay-ups B and C). Fig 2 shows the importance of the test configuration in measuring compression strengths: the anti-buckling guide, used in phase 1 and described in Ref 1, gave values similar to those for the short unsupported specimens when used in a very rigid 500kN test machine, but the same anti-buckling guide used in a smaller less rigid machine gave values significantly lower.

5 IMPACT TESTS

Most of the work on impact damage used the dropweight technique from phase 1 which is described in Ref 1. The laminates were clamped horizontally over a 100mm internal diameter circular steel support. The impactor, with a nose diameter of 10 mm was dropped through 1 m (impact velocity 4.43 m/s) onto the centre of the unsupported area. The incident energy was altered up to 6 J by adjusting the mass of the impactor.

In addition ONERA varied the area supported, from fully supported to 100 mm diameter, and the drop height from 0.25 m (2.2 m/s) to 4 m (8.9 m/s). DFVLR did some work with a modified instrumented dropweight apparatus, comparing single impacts with repeated impacts, and varying the materials and the drop height. Fig 4 shows comparisons between single impacts and repeated impacts for various energies, and the effects on maximum deflection and force, on duration of impact and maximum force during impact. The repeated impact was continued until penetration occurred. In general the repeated impacts produce more damage and greater reductions in stiffness, for the same incident energy. Figs 5 to 9 show similar tests on a $[0,90]_6$ fabric laminate and on $[0,90,\pm 45,0]_s$ laminates for which carbon fibre plies are replaced by glass fibre plies or by carbon fibre/aramid. The use of carbon fibre fabric reduces both the load carrying capacity and the energy absorption during impact. The glass fibre laminate was able to absorb about four times as much energy as the carbon fibre laminate before penetration. Fig 10 shows that replacing only a few of the carbon fibre plies by glass fibre plies to form hybrid laminates results in significant increases in energy absorption, the best hybrid tested being when the 45 deg plies were glass fibre. The smaller increment in energy was able to differentiate between the hybrids much better than the larger impact energy. Fig 11 shows that the [illegible]

fabrics results in less energy absorption. Fig 12 shows the penetration energies for all the various laminates tested, again showing the benefit of glass fibres and the slight embrittlement produced by carbon fibre fabrics.

6 IMPACT DAMAGE

The damage caused by the dropweight impact on the various laminates is shown in Figs 13-25. In Fig 13, front and back face views are given of damage caused by incident energies of 2-12 J on the NLR base carbon fibre laminate and on the base laminate with face sheets of aramid, glass or carbon fibre fabrics. The base laminate showed extensive splitting on the back face at 10 J so the 12 J impact was not carried out. The fabric face sheets all restricted the area of damage on the back face. In the ARALL material there was cracking of the Al sheet at incident energies greater than 6 J (Fig 14).

Figs 15 and 16 show examples of the damage produced by the DYNATUP impact testing. The restriction of the damage by fabric is shown in Fig 15. The glass fibre laminate in Fig 16 is translucent and one can see, in addition to the back ply splitting, the delaminations between the various plies. The hybrid shown in Fig 16, when compared with the similar all-carbon fibre laminate of Fig 15, shows how surface plies of higher strain fibres can prevent fibre breakout on the back face.

Figs 17 and 18 show ultra-sonic C-scans of the NLR laminates. These confirm the restriction by the fabrics of back ply splitting but they show that the areas of internal delamination are about the same. Cross section through the damaged regions (Fig 19) show that although the areas of damage appear to be similar the damage is less severe in the fabric faced sheets. The delaminations in the ARALL were small in extent due no doubt to the thoughness of the adhesive.

Figs 20 and 21 show ONERA C-scans comparing damage in 914 and 5208 laminates. The areas of damage were very similar in the two materials. The orientations of the C-scan patterns show how the delaminations extend in the directions of the fibres, whose stiffness in these directions allows significant transfer of stress.

DEVIE has carried out areas of delamination and broken fibres in Figs 22 and 23, for the various fabric and hybrid laminates. This shows that straight carbon fibres produce the greatest extensions of delamination, whereas the carbon fibre fabric restricts the area of damage but causes it to be more severe in terms of broken fibres. The glass fibres, being less stiff and having greater strain capacity to failure, restrict both the area of delamination and the number of broken fibres.

[illegible] and [illegible] show the effects, on areas of damage, of varying the impact conditions. The [illegible] supported specimens were not able to flex and therefore experienced [illegible] applied compressive loads with few [illegible] tensile [illegible] supports allowed relatively large volumes of material [illegible], keeping the stresses low and mainly in-plane. [illegible] damage, as there was less extensive elastic deformation, [illegible] stresses, and having a greater depth-to-span ratio the [illegible] would have been more prominent. The effect of impactor [illegible] studied [illegible], the important parameter [illegible]. However, there was [illegible] was approaching [illegible] where the [illegible]

[illegible]

[illegible]

[illegible] strains [illegible]

[illegible] demonstrates the [illegible] impact damage on static strengths [illegible] the importance of the stabilising [illegible] when [illegible] have reasonable [illegible] these particular specimens the [illegible] stability [illegible]

[illegible] laminates [illegible], with [illegible] the [illegible] the [illegible] fibres, while not affecting the [illegible] strengths of the undamaged specimens, [illegible] tensile strength after impact. [illegible] would promote [illegible] splitting, making the specimens less notch sensitive in tension. This is supported by the [illegible] Fig. [illegible], the results are not [illegible]

9 RESIDUAL FATIGUE PROPERTIES

ONERA compared the residual tatigue properties of T300/5208 graphite/epoxy specimens with drilled holes, at two loading conditions, for [90/±45/0]$_{2s}$, [90$_2$/±45]$_s$ laminates (Fig 38), the quasi-isotropic laminate had a greater compressive strength than the other laminate but the S-N curve so that at 10^5 cycles there was little difference. Reversed loading (R = -1) was more detrimental than the repeated compression loading (R = 10), especially for the specimens with the thicker laminate. For the [+45$_2$/-45$_2$]$_s$ laminates (Fig 39), the impacted and the drilled specimens had similar strengths but, on fatigue, the reversed loading was more severe than the repeated compression loading. Similar results were obtained with the T300/5208 (Figs 39 and 40) except that in the case of the [90$_2$/90$_2$]$_s$ laminate had a slightly steeper S-N curve under reversed loading.

Fig 41 shows the effect of test frequency on the fatigue life of the matrix dominated [+45$_2$/-45$_2$]$_s$ laminates. With the exception of the 10 Hz frequencies showed slightly better fatigue lives, probably due to viscoelastic tendencies or other relaxation effects. Differences in life were there was less scatter.

Fig 42 shows the results on a [45/0/-45/90]$_{2s}$ laminate, the S-N curve for R = -1 was used to obtain residual strength properties.

Fig 43 shows the effect of test temperature on the fatigue performance of notched and unnotched specimens. The results of the tests showed significant reductions in static and fatigue strength at the 93°C curves crossed to much greater extent in the notched specimens. This was due to the combination of the thermal stresses and the stress concentration effects at the notch. Fig 44 shows the effect of moisture on a variety of lay-ups. Most of the tests were carried out at 71°C which is the worst case for metal bonding.

10 DISCUSSION

The test results presented in this section are typical of the performance of the composite materials. The fatigue resistance of a particular component would be dependent on the design and in particular on its dynamic response.

In compressive testing, the design of the anti-buckling guide and the rigidity of the load train were critical in determining whether failure was caused by compressive failure of the material or by an instability. Either failure mode could be important in structural components.

The laminate lay-up or ply stacking sequence had a significant effect on test results. When the 0 degree plies were blocked together, $[(\pm 45)_2 0_2]_s$, the laminate had the best ultimate tensile strength and a good residual tensile strength after impact. This was because the 0 degree splitting blunted the crack and relieved the stress concentration. However, in compression the splitting promoted local instability and precipitated premature failure. Under static loading, at applied strains of about 0.4%, the 0 degree splitting was able to cause delamination to grow with them. Laminate sequences with the 0 degree plies better in compression but were more [illegible] section showed the influence of the 45 degree plies on the [illegible] sections was with the intermediate dispersion [illegible].

[illegible] with carbon fibre fabric at 45 degrees had definite [illegible] the ultimate tensile strength of the intermediate dispersion [illegible] by about 40%, while having little effect on the compressive [illegible]. Ultrasonic tests and polished cross sections showed that the fabric [illegible] the extent of impact damage. This reduced the penetration [illegible] but increased the residual strength, especially in compression. The [illegible] also inhibited the growth of damage under tensile loading at 0.4% strain.

The glass fibre fabrics gave an increase of four times in the energy absorbed during impact, improving the penetration resistance. It also restricted the extent of impact damage so that although the initial compression strengths were relatively poor, the residual compression strengths after impact were good.

The aramid fibre fabrics restricted the extent of impact damage, as did the other fabrics, but the residual compressive strengths were not improved.

There was some indication, from the limited number of resin matrices tested, that tougher resin systems improved the impact performance.

The ARALL behaved more like a metal than a fibre reinforced composite. The plasticity of the fibre enabled it to absorb much of the impact energy and to restrict the damage, with little delamination. However, there was still some cracking in the alloy sheets and this propagated under subsequent tension loading. The glass fibre was found to be the most suited fibre.

In the laminates containing 0 degree plies the strains were small. Stress concentrations from machined notches or impact damage caused a marked reduction in the static strengths. Subsequent fatigue however produced relatively flat S-N curves. The strains needed to cause fatigue growth were close to those which produced static failures. In (±45) laminates the working strains were greater, and the S-N curves were steeper. In this case the stress ratio was important, reversed loading being more detrimental than compression-compression loading.

The results indicate that the static properties of fibre reinforced composites are significantly affected by localised stress concentrations like notches or impact damage, whereas the fatigue properties are more dependent on the intrinsic properties of the laminates. If the static problems are alleviated and the working strains increased, then fatigue may become more of a problem.

Most of the information on the impact performance of fibre reinforced composites is empirical. There are sufficient data to draw some general qualitative conclusions, but there is a need for quantitative predictive techniques, both of the damage formation and of its effect on residual properties.

There is also a need for improved materials. Some improvements can be made by altering lay-ups and using hybrid laminates, but greater advances should come from materials developments and from the imaginative combinations of materials in hybrid structures.

11 CONCLUSIONS

The work undertaken in phase two of this programme confirmed the findings of phase one, *that impact damage in carbon fibre reinforced composite laminates* can reduce the static strengths and low cycle fatigue strengths significantly, especially the compressive strength. However, subsequent fatigue loading produces flat S-N curves and high cycle fatigue strengths are similar to those for undamaged laminates.

Some improvements can be made to the impact performance by optimising laminates lay-ups and by the use of surface plies of carbon or glass fibre fabrics.

More significant improvements in the residual static strengths should come from improved materials properties, such as fibre, matrix and interface properties, and from improved structural design. This may result in increased fatigue sensitivity.

There is a need for quantitative techniques to predict the formation of the damage and the residual strengths.

Table 1

GARTEUR SM/AG01 PHASE 2 PROGRAMME

	RAE	NFRA/CEAT	NLR	DFVLR
Material	T300/914 Carbon/Kevlar Carbon fabric	T300/914 T300/5208	T300/914 Carbon/Kevlar- Glass fabric ARALL	T300/914 T300/Code 69 Carbon/Glass
Lay-up	$[(\pm 45)_2\ 0_4]_S$ $[+45\ 0\ -45\ 0]_S$	$[(\pm 45)_2\ 0_4]_S$ (0, 90) (±45)	$[(\pm 45)_2\ 0_4]_S$	$[(\pm 45)_2\ 0_4]_S$ (±45, 0, 90) $[\pm 45, 0_2, 90, 0]_S$
Specimen size	250 × 50	250 × 50 and others	250 × 50	250 × 50
Damage	Undamaged Dropweight C-scan	Undamaged Machined holes	Undamaged Dropweight C-scan	Undamaged Dropweight C-scan
Static tests	Vary strain rate			
Fatigue tests	R = -1	R = -1 Damage growth C-scan X-rays Acoustic emission	R = -1	R = -1

Table 2

PROGRAMME OF WORK AT ONERA-CEAT

1 Mechanical testing.

Materials	Lay-ups	Specimens	Tests
T300/914	$[(\pm 45)_2, 0_4]_s$	250 mm · 50 mm	Static tension
T300/5208	$[0_2, 90_2]_s$	5 mm drilled hole	Compression
	$[+45_2, -45_2]$	Impacted	Fatigue 2 Hz R = -1 R = -10

2 Determination of the impact energy to obtain damaged area of about 5 mm diameter.

3 Effect of the support geometry during impact.

4 Effect of the velocity of the impactor for a given energy.

5 Effect of frequency for $[+45_2, -45_2]_s$ specimens.

6 Damage monitoring, after impact, during fatigue loading.

Table 3

LAMINATES TESTED AT DFVLR

[0/90/±45/0] sym. w w fab. w	
[0/90/±45/0] sym. fabr. w w	
[0/90] 6x fabric	
[0/90/±45/0] sym. c c c c	
[0/90/±45/0] sym. g g g g	
[0/90/±45/0] sym. c c c g	
[0/90/±45/0] sym. c c g c	
[0/90/±45/0] sym. c g c c	
[0/90/±45/0] sym. g c c c	

c indicates carbon fibre T300

g indicates E-glass fibre

w indicates warp sheet

fab. indicated fabric

Table 3

PROGRAMME OF WORK AT RAE

1 Laminates.

Laminate	Lay-up	Specific Results
A	[illegible]	[illegible]
[illegible]	[illegible]	[illegible]
[illegible]	[illegible]	[illegible]
[illegible]	[illegible]	[illegible]
[illegible]	[illegible]	[illegible]
[illegible]	[illegible]	[illegible]
[illegible]	[illegible]	[illegible]
[illegible]	[illegible]	[illegible]
[illegible]	[illegible]	[illegible]
[illegible]	[illegible]	[illegible]

[illegible]

Table 5

BASIC PROPERTIES OF THE LAMINATES TESTED AT NLR

Material	Weight kg/m^2	E* GPa	σ_{max} MPa	ε_{max}	t mm
Base lam.	2.95	78.0	970	1.18	1.9
ARALL	3.62	65.0	845	2.50	1.5
base lam. + $Ca_{\#}$ fabric	3.46	66.0	823	1.26	2.3
Base lam. + $Glass_{\#}$ fabric	3.74	64.9	800	1.22	2.5

* Secant modulus at ε = 0.003

fabric in sheet at 45° with test direction

Table 5

TEST RESULTS FROM NLR ON (a) BASE LAMINATE; (b) BASE LAMINATE PLUS GLASS FABRIC FACE SHEETS; (c) BASE LAMINATE PLUS CARBON FABRIC FACE SHEETS

(a) Laminate type	Number	Impact energy (J)	Fatigue, R = -1 P kN	Fatigue, R = -1 ε	$\Sigma_{(tot)}$ kc	Residual compressive strength P_{max} kN	σ_c MPa	ε %	$A_{initial}$ mm²	$A_{+n\,cycles}$ mm²
	7	-				57.8	608	0.78	-	-
	8	-				63.0	662	0.85	-	-
Base	9	5				46.0	484	0.62		
laminate	10	5				43.5	458	0.59		
	5	5	27.5	0.37	500	48.0	502	0.64		
$(\pm 45_2, 0_4)_s$	6	5	27.5	0.37	500	55.5	582	0.75	190	780
	1	5	30.0	0.40	51	48.6	511	0.65	150	1530
	2	5	30.0	0.40	100	54.5	572	0.73	280	1160
	3	5	30.0	0.40	100	37.9	400	0.51	210	2300
	4	5	32.5	0.44	100	58.0	610	0.79	220	1020
	11	3.75	32.5	0.44	100	44.9	472	0.60	90	>10580*
	12	3.75	32.5	0.44	100	48.4	510	0.65	50	> 970*

*delamination area at 10^4 cycles

Table 6 (continued)

(b)

Laminate type IV	Number	Impact energy (J)	Fatigue, R = -1 P kN	ε %	N_{total} kc	Residual compressive strength P_{max} kN	σ_c MPa	ε %	$A_{initial}$ mm^2	$A_{fatigue}$ mm^2
	7	-				69.0	600	0.93		
Base	8	-				72.7	630	0.97		
laminate	10	5				54.6	474	0.73	250	
	9	5				47.9	417	0.64	280	
+	5	5*	27.5	0.37	500	72.4	630	0.97		
	6	5	27.5	0.37	500	51.0	443	0.68		
Glass	1	5	30.0	0.40	50	37.7	328	0.51	270	2860
fabric	2	5	30.0	0.40	100	53.9	470	0.72	350	350
	3	5	30.0	0.40	100	44.8	390	0.60		
	4	5	32.5	0.44	100	52.2	455	0.70		
	12	5	32.5	0.44	100	52.4	455	0.70	280	280
	13	5	32.5	0.44	100	46.0	400	0.62	250	250

*no detectable initial impact damage

Table 6 (concluded)

(c)

Laminate type III	Number	Impact energy (J)	Fatigue, R = -1 P kN	Fatigue, R = -1 ε %	N_{total} kc	Residual compressive strength P_{max} kN	Residual compressive strength σ_c MPa	Residual compressive strength ε %	Residual compressive strength $A_{initial}$ mm^2	Residual compressive strength $A_{fatigue}$ mm^2
	7	-				75.1	653	0.99		
Base	8	-				77.0	670	1.02		
laminate	9	5				56.2	490	0.74	240	
+	10	5				56.0	487	0.74	220	
	5	5	27.5	0.36	500	49.5	430	0.65		
Carbon	6	5	27.5	0.36	500	56.5	491	0.74	240	250
fabric	1	5	30.0	0.40	100	45.8	397	0.60	230	410
	2	5	30.0	0.40	100	63.6	550	0.86	320	350
	3	5	30.0	0.40	100	29.9	261	0.40	310	350
	11	5	32.5	0.43	100	51.6	450	0.68	210	280*
	12	5	32.5	0.43	100	62.2	540	0.80	260	290*
	13	5	32.5	0.43	100	56.0	486	0.74	210	280*

*delaminated area after 10^4 cycles

Table 7

CHANGE IN LENGTH MEASUREMENTS, IN mm, OVER THE LOAD RANGE 7-39 KN (NLR)

Sp. nr	Number of cycles							
	0	10^3	10^4	5.10^4	10^5	2.10^5	5.10^5	
I 1	196		227	230				
				224*				
I 3	203	205	208					
		199	215					
I 4	195	200	211		215			
		192	210					
I 5	185	214						
I 6	188		189		205	206	206	
			189		200			
III 1	182		186	190	197			
			186	190				
III 3	195	192	191		200			
		191	192					
III 4	180	184	188		192			
	182	184	188					
III 5	200	200						
III 6	194		196		197	195		
			197		195			
IV 1	188		192	208				
				210				
IV 3	194	196	196		197			
		192	199					
IV 4	186	186	191		194			
		189						
IV 6	191		194		195			
			197					

*Measurement repeated after mounting the specimen again in the fatigue machine

REFERENCES

No.	Author	Title, etc.
1	G. Dorey P. Sigety K. Stellbrink W.G.J. 't Hart	Impact damage tolerance of a carbon fibre composite laminate. RAE Technical Report 84049 (1984) CARTEUR TP-60.
2	P. Sigety	Impact damage tolerance of composite materials. Progress Report of ONERA-CEAT work up to Oct [illegible].
3	W.G.J. 't Hart	Impact/fatigue performance of a $[(\pm 45/0_2/90_2)_3]_s$ high carbon/epoxy laminate. NLR Technical Report 85108 L (1985)
4	K. Stellbrink	Effect of hybridization on impact behaviour of CFRP laminates. DFVLR Draft, 20 September 1985
5	K. Stellbrink H.M. Aoki	Effect of defect on the behaviour of composites. ICCM-IV, Tokyo (1982)

Fig 1

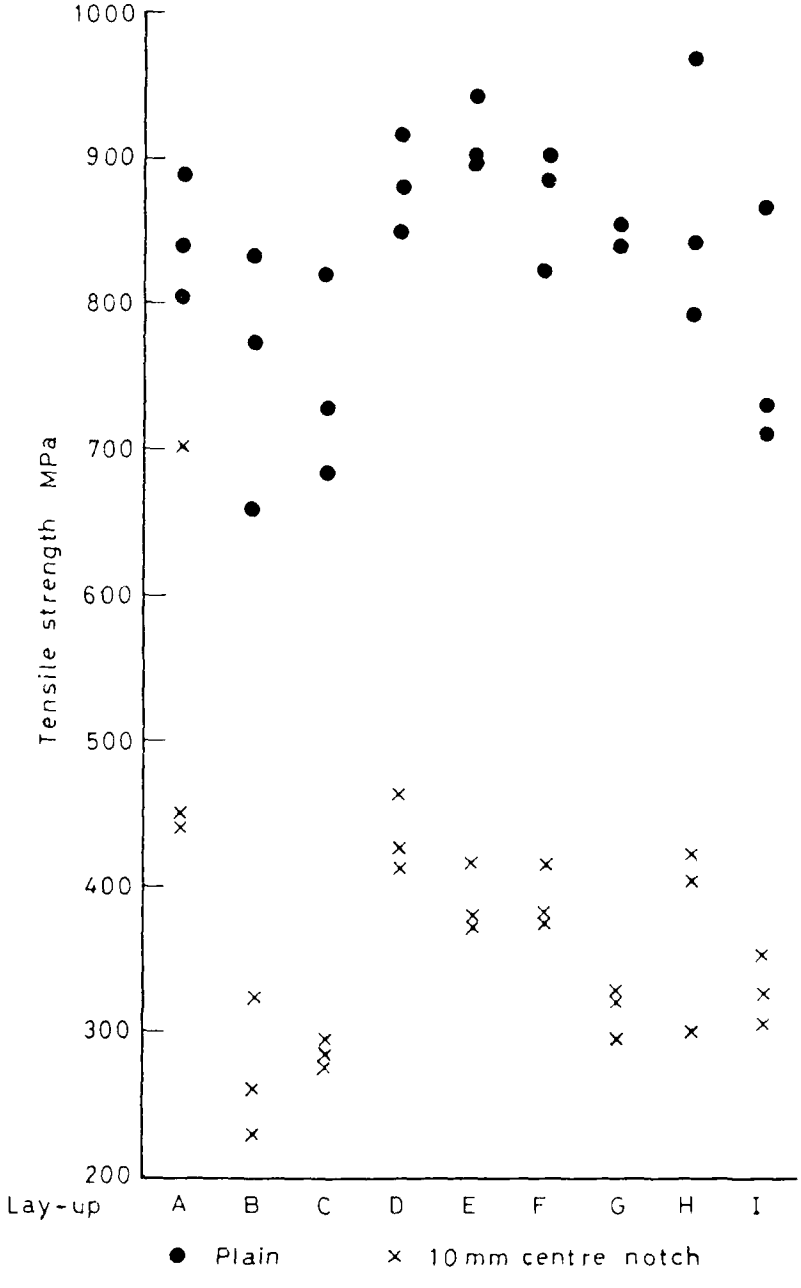

Fig 1 Tensile strengths or carbon fibre laminates, 2 mm thick, plain unnotched or notched (RAE)

Fig 2

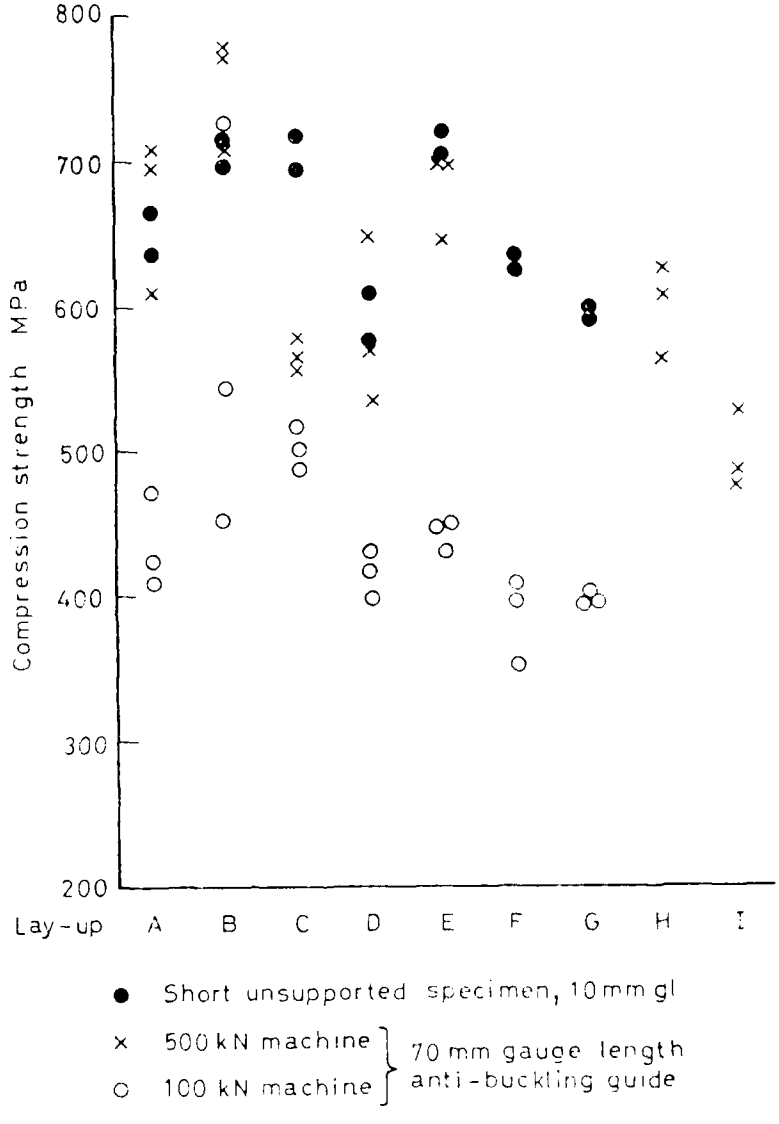

Fig 2 Compressive strengths of carbon fibre laminates, 2 mm thick, with different stabilising conditions (RAE)

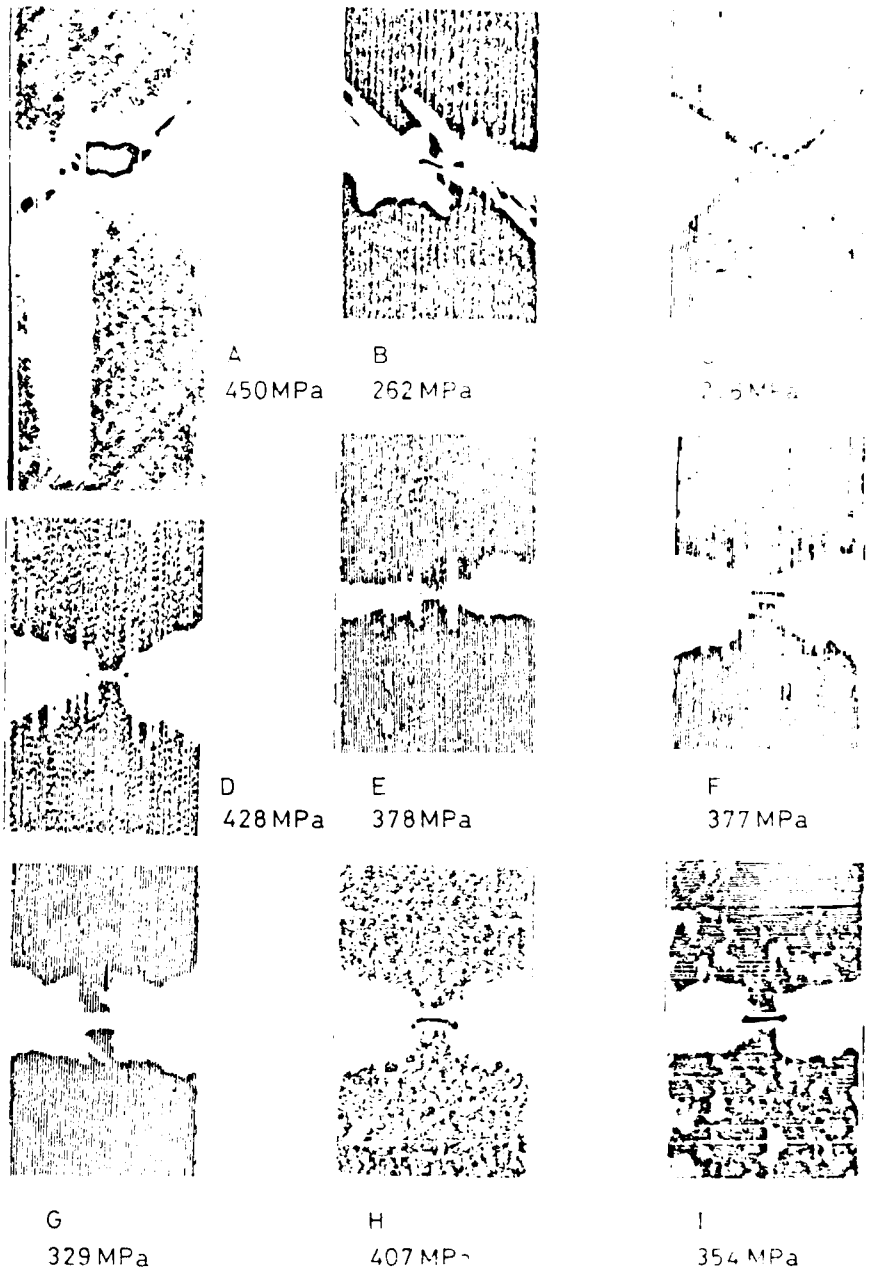

Fig 3 Ultrasonic C-scans of notched tensile specimens of various (0, 45) carbon fibre laminates (RAE)

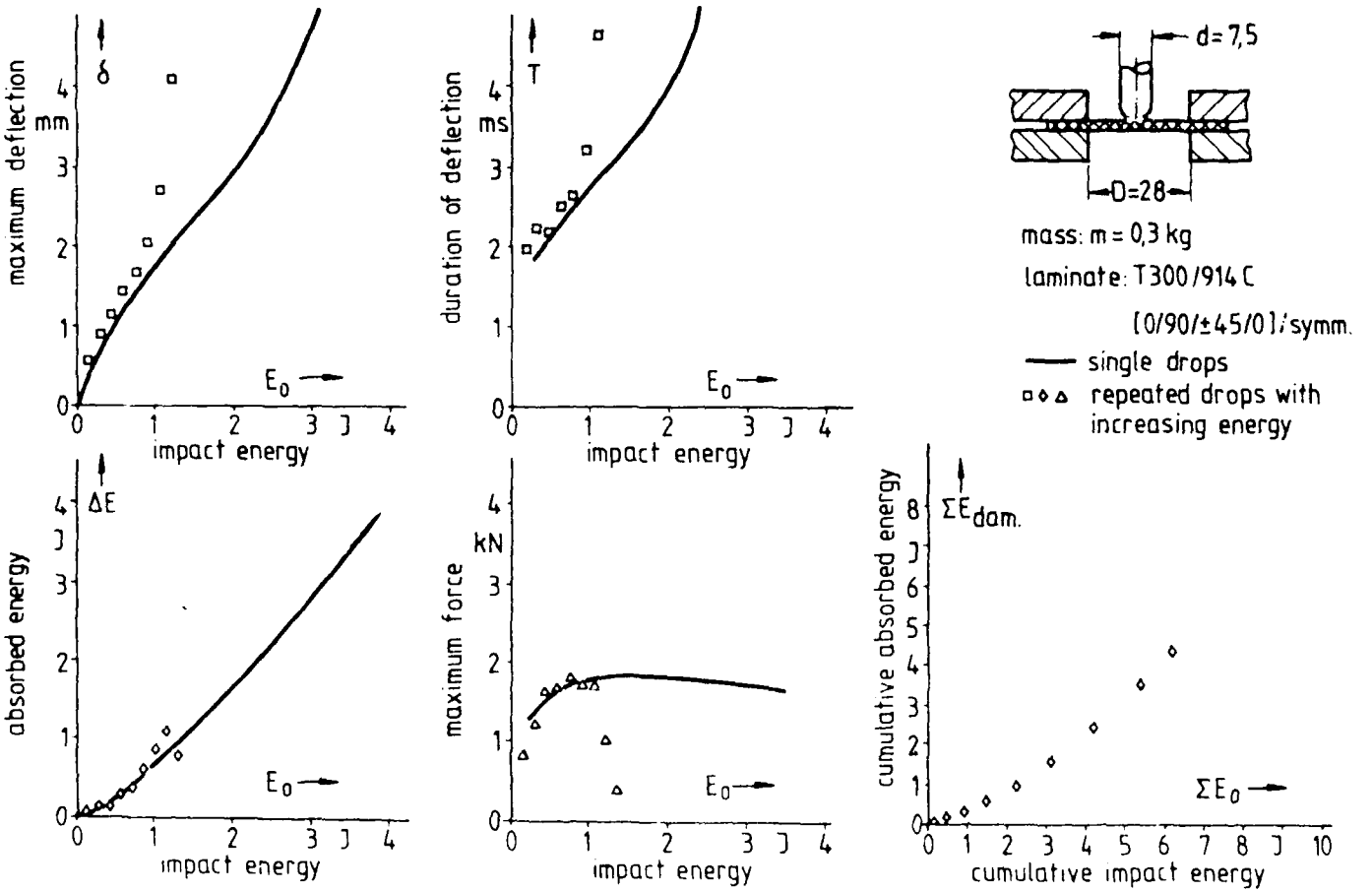

Fig 4

Fig 4 Measured parameters from instrumented dropweight impact tests on a CFRP laminate (DFVLR)

Fig 5

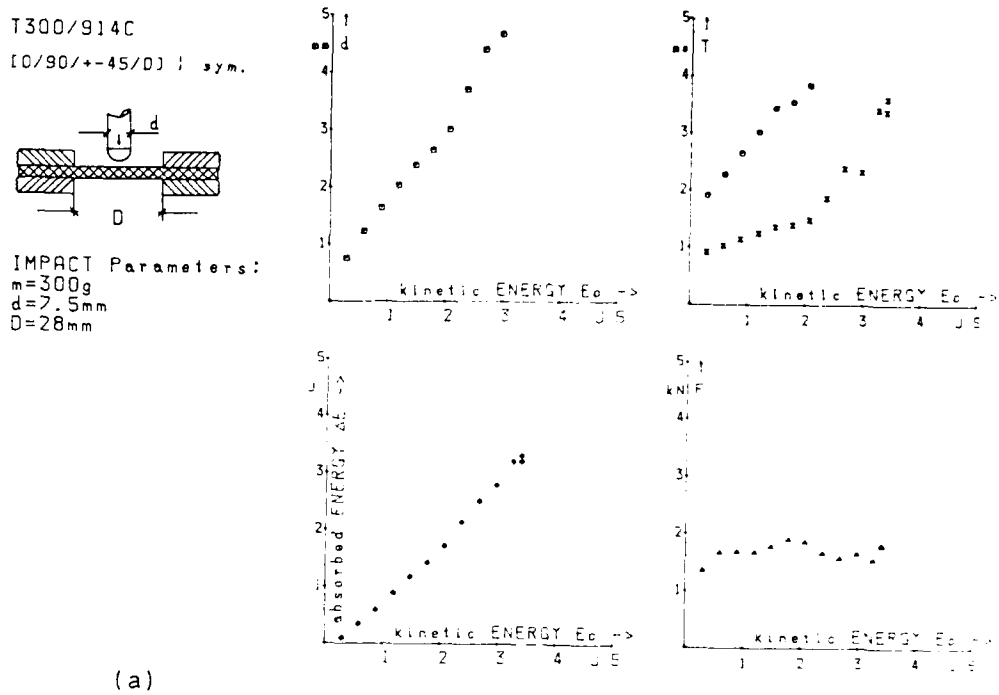

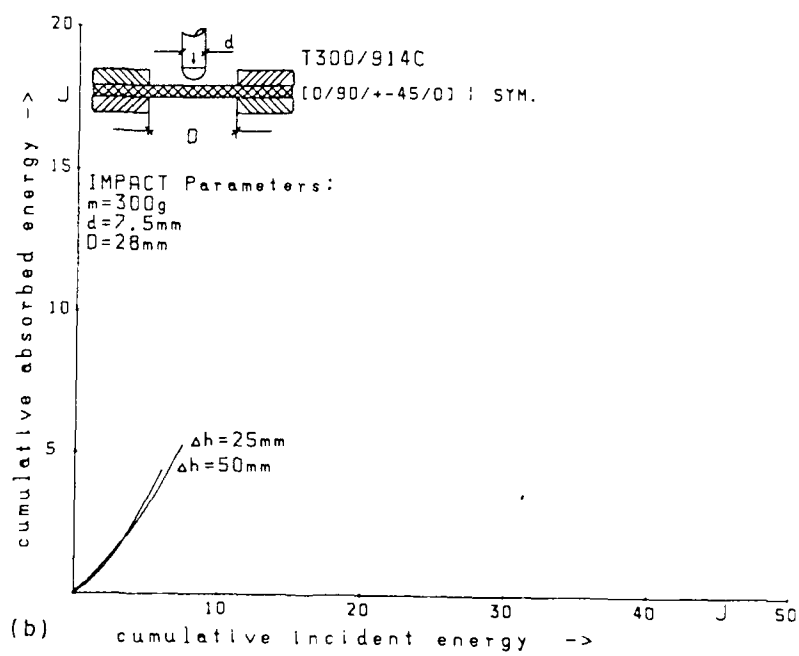

Fig 5 Energy absorbed during dropweight test on a CFRP laminate
(a) single drop
(b) repetitive drop (DFVLR)

Fig 6

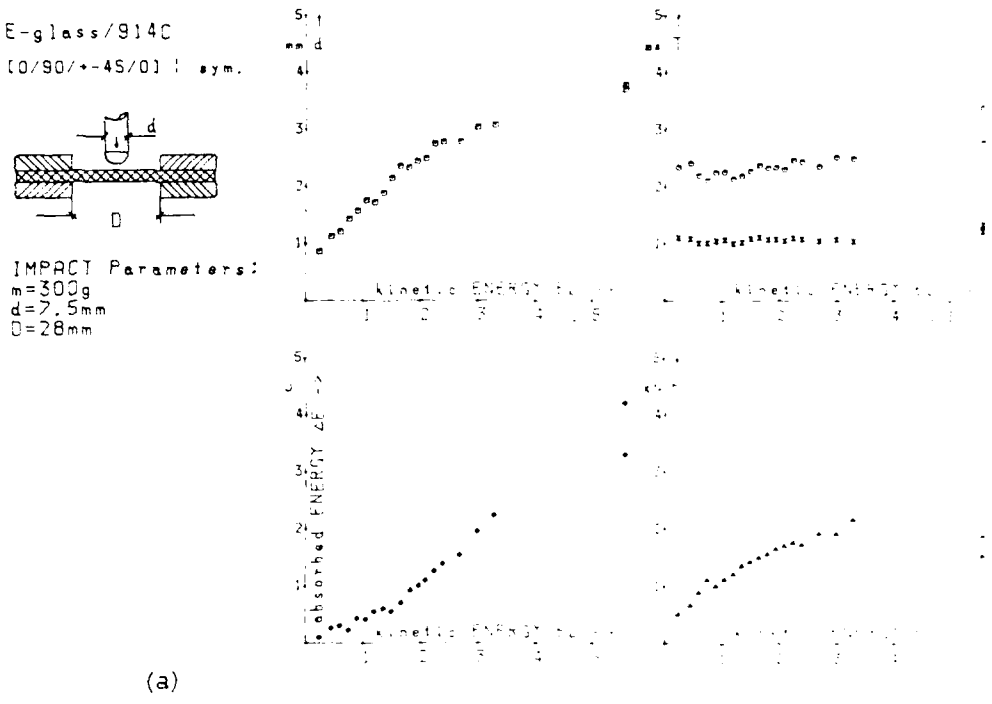

(a)

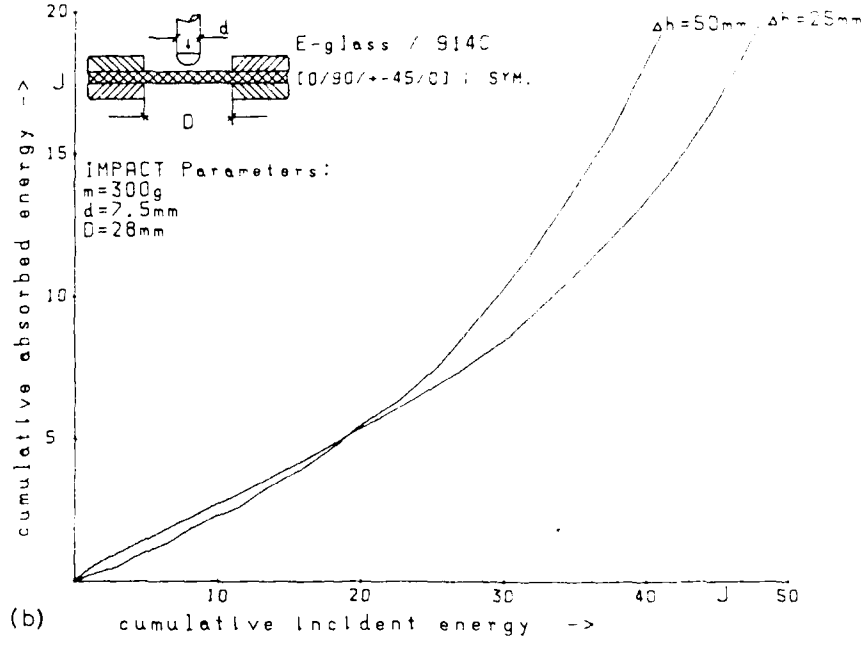

(b)

Fig 6 Energy absorbed during dropweight test on a GRP laminate
(a) single drop
(b) repetitive drop (DFVLR)

Fig 7

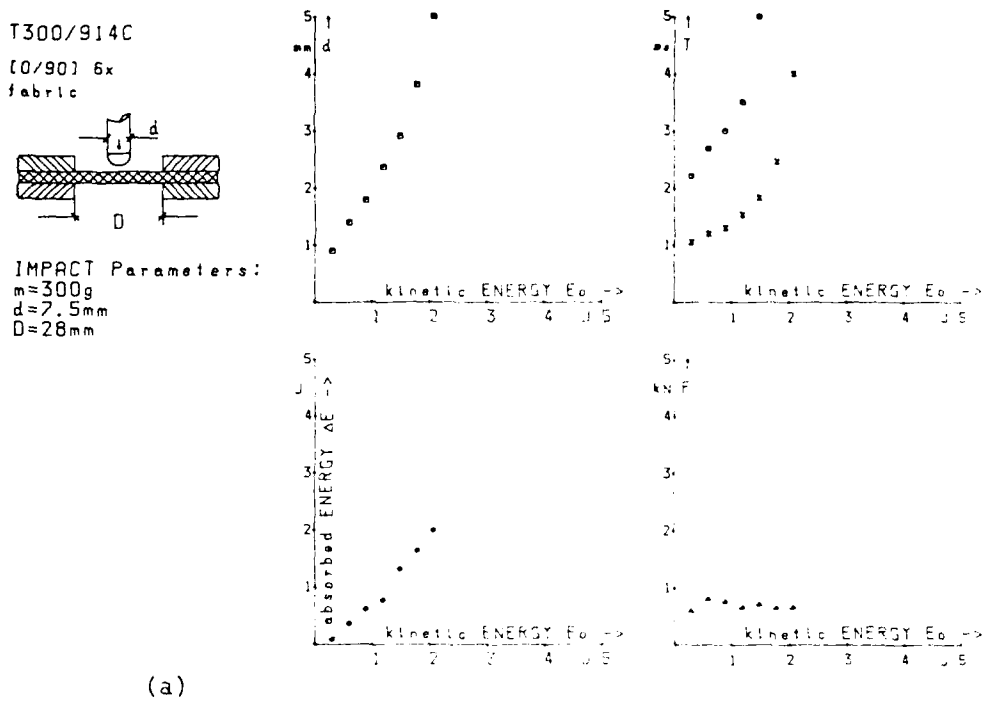

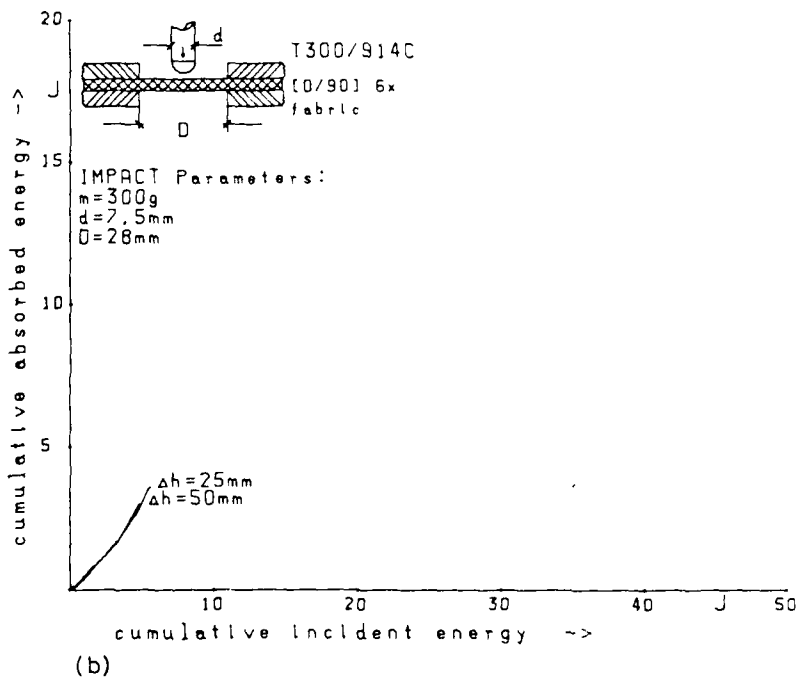

Fig 7 Energy absorbed during dropweight test on a CFRP fabric laminate
(a) single drop
(b) repetitive drop (DFVLR)

Fig 8

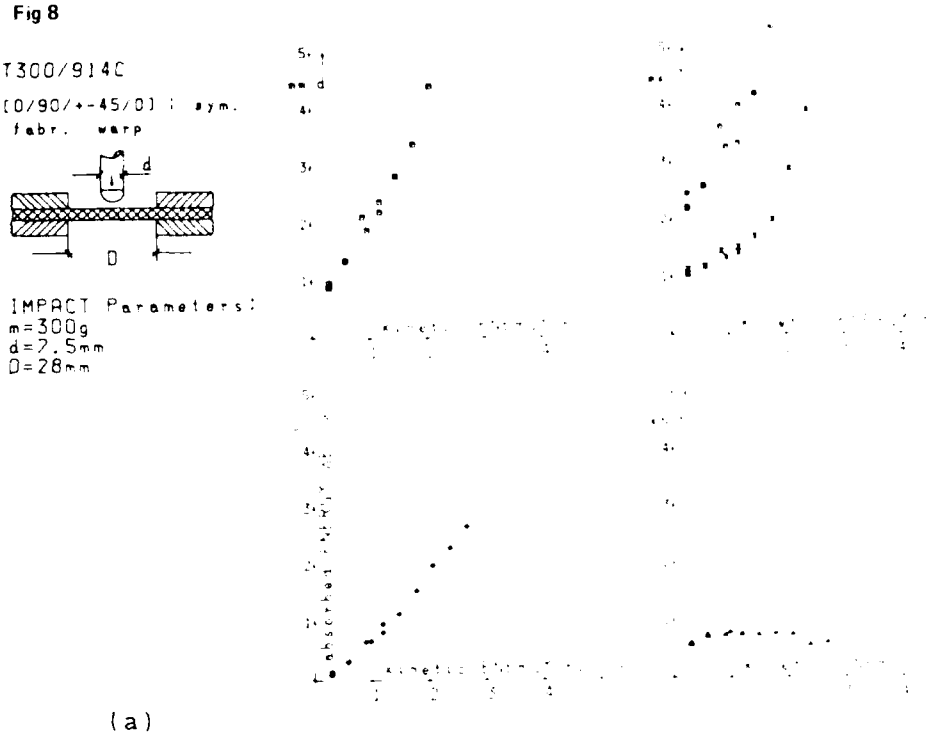

(a)

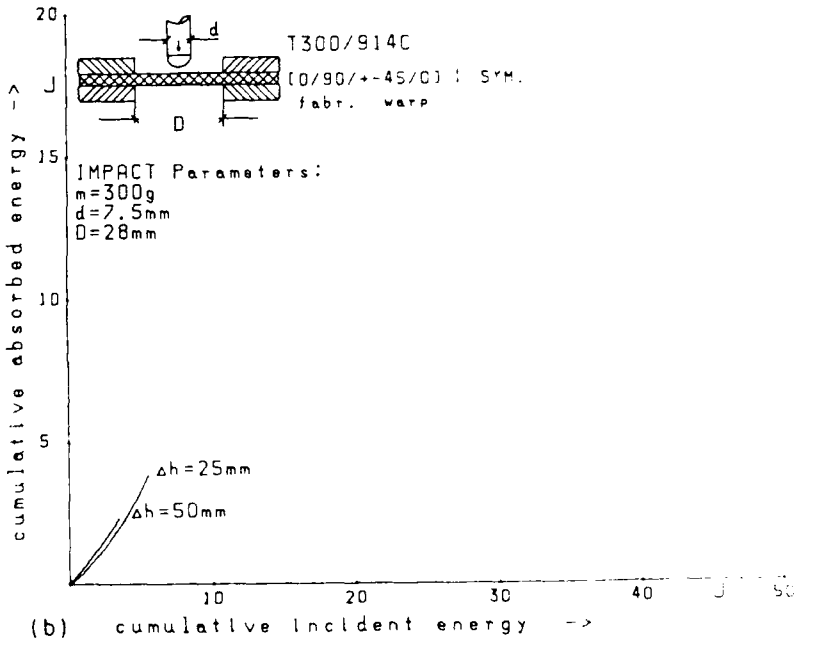

Fig 8 Energy absorbed during dropweight test on a CFRP mixed warp/fabric laminate
(a) single drop
(b) repetitive drop (DFVLR)

Fig 9

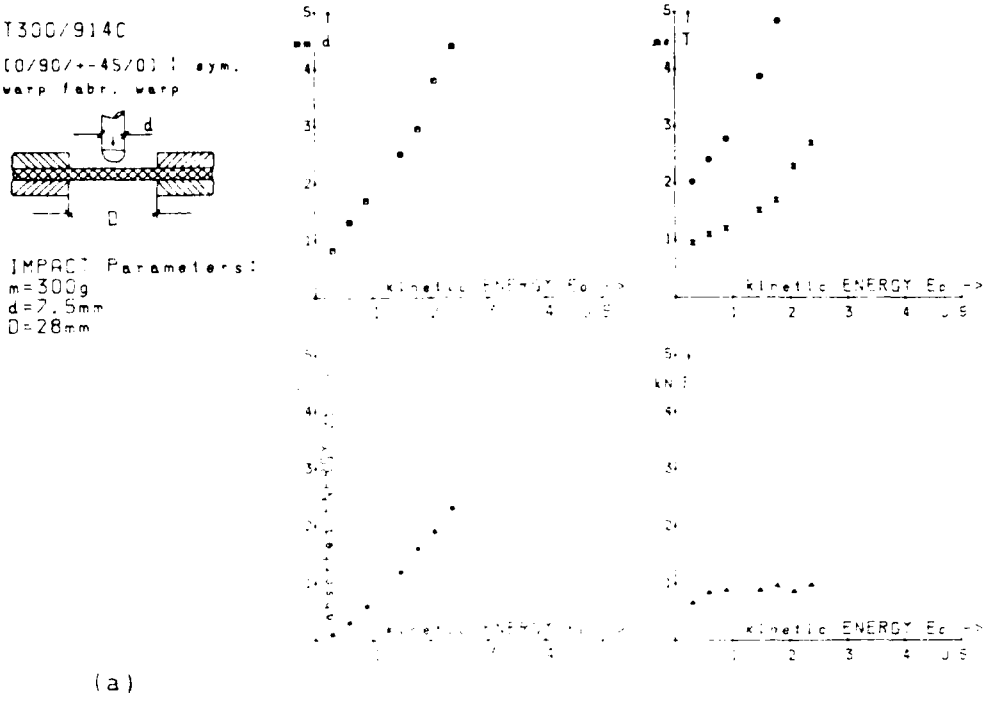

(a)

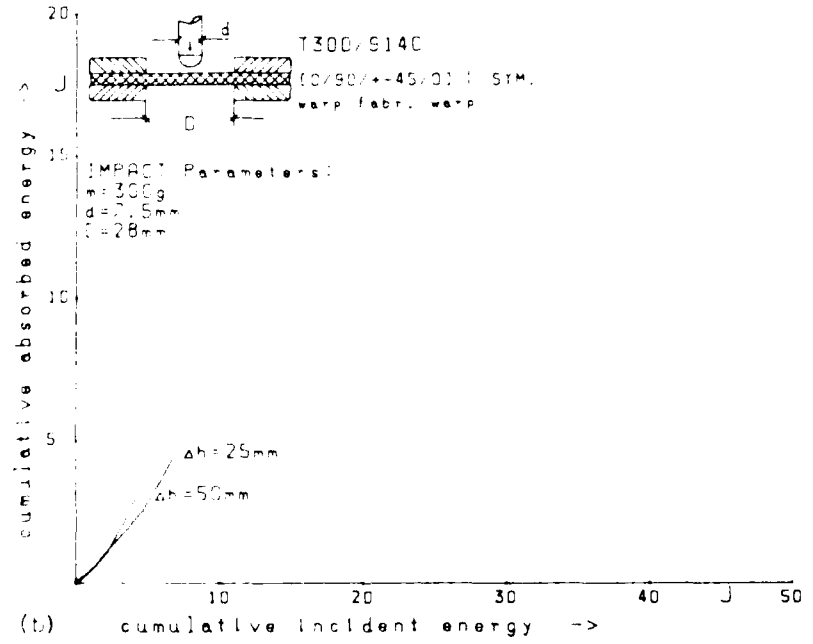

(b)

Fig 9 Energy absorbed during dropweight test on a CFRP mixed warp/fabric laminate
(a) single drop
(b) repetitive drop (DFVLR)

Fig 10

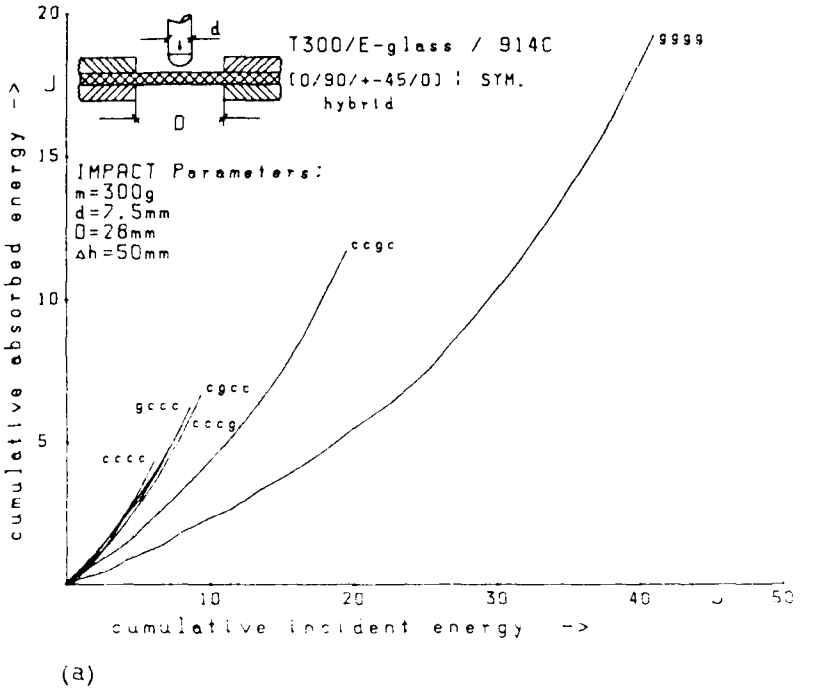

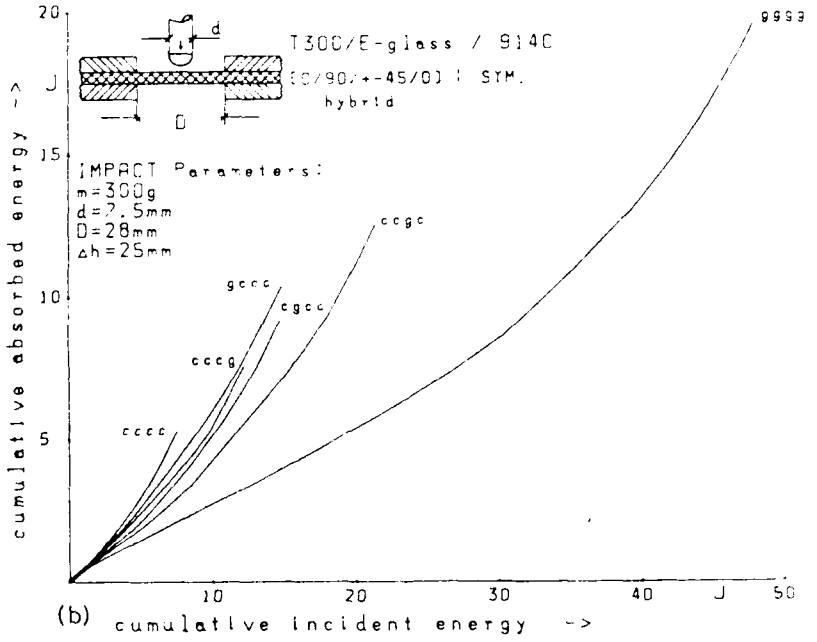

Fig 10 Energy absorbed during repetitive dropweight tests on carbon/glass hybrid laminates, with increments in drop height of
(a) 50mm
(b) 25mm (DFVLR)

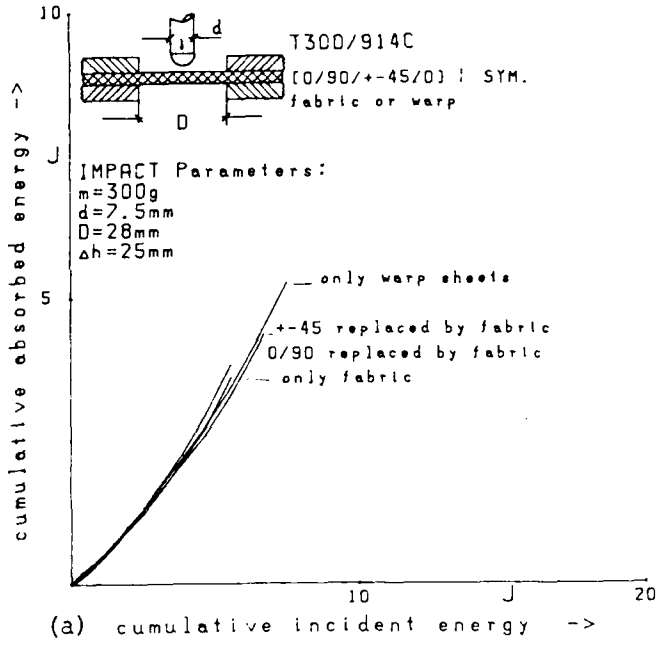

Fig 11 The effect of carbon fibre fabric plies on the energy absorbed during repetitive dropweight tests on CFRP laminates (DFVLR)

Fig 12 Incident energies to cause penetration in single and repetitive dropweight tests on various CFRP, GRP and hybrid laminates (DFVLR)

Fig 13

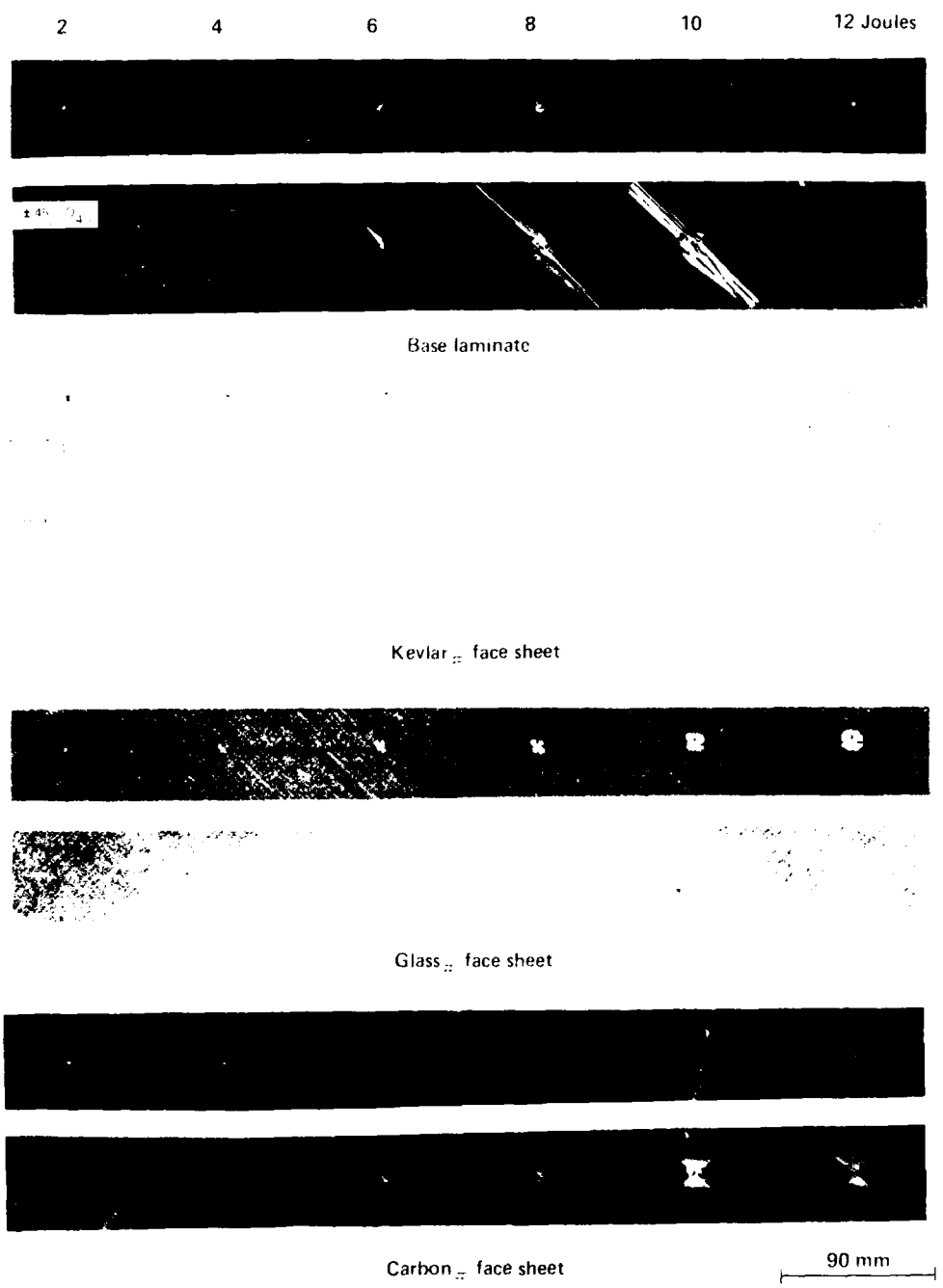

Fig 13 Photographs of impact tested laminates (NLR)

2 4 6 8 10 12 Joules

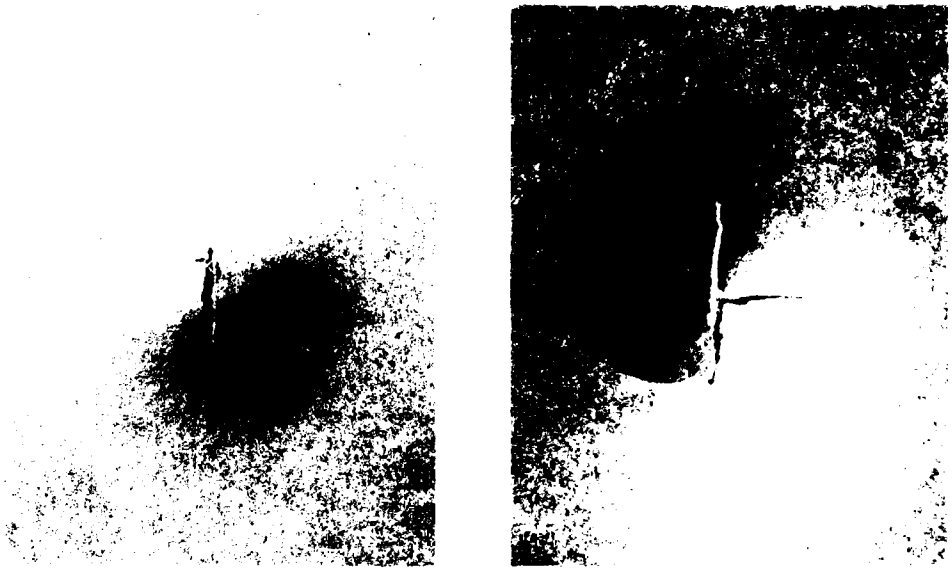

8 Joules 10 Joules

5 mm

Fig 14 Impact damaged ARALL laminate and details of crack formation in the back face sheet (NLR)

Fig 15

T300/914C

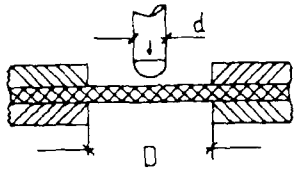

IMPACT Parameters:
m=300g
d=7.5mm
D=28mm

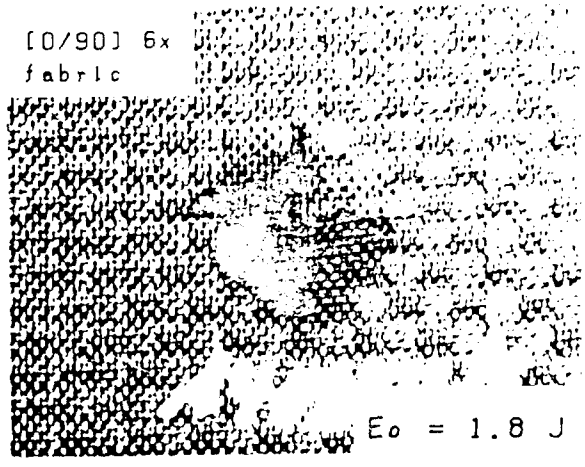

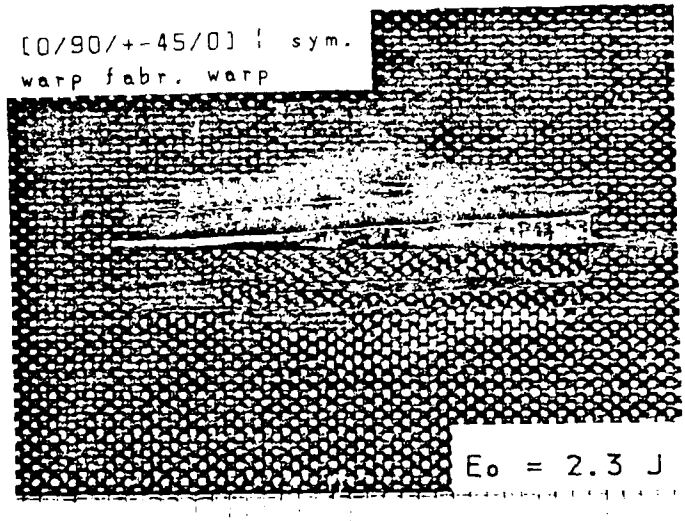

3 4 5 6

magnification: 3 X

Fig 15 Impact damage in CFRP fabric and mixed warp/fabric laminates (DFVLR)

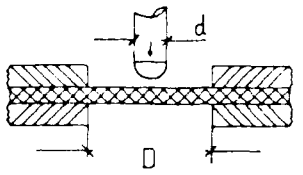

IMPACT Parameters:
m=300g
d=7.5mm
D=28mm

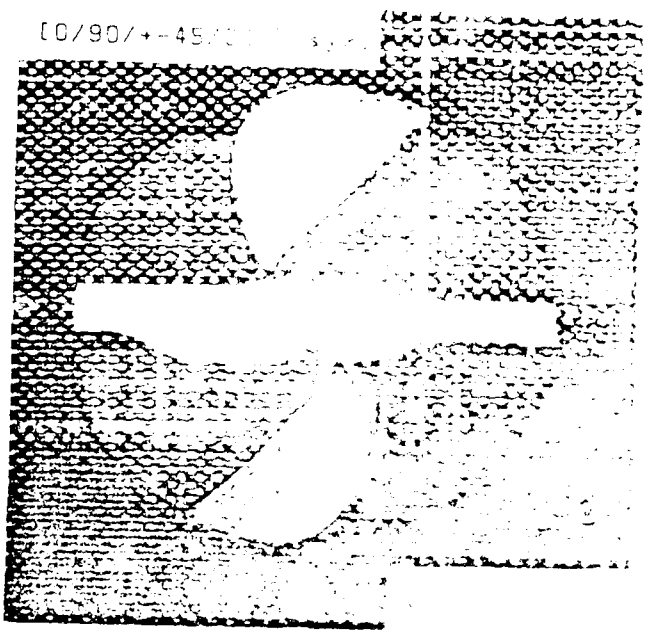

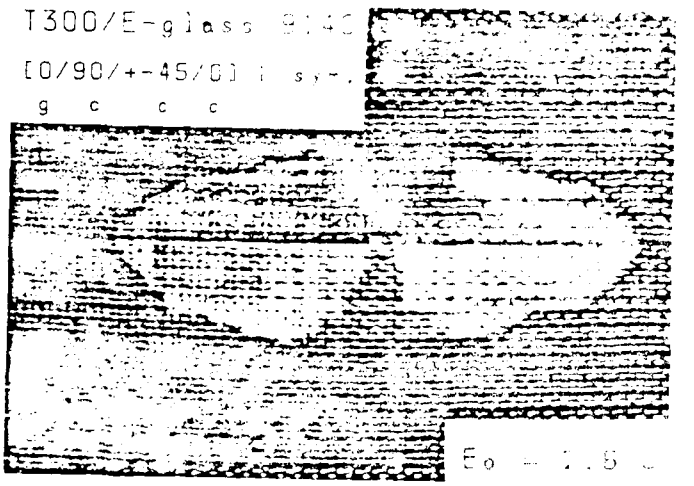

magnification: 3 X

Fig 16 Impact damage in GRP and CFRP-GRP hybrid laminates [14]

Fig 17

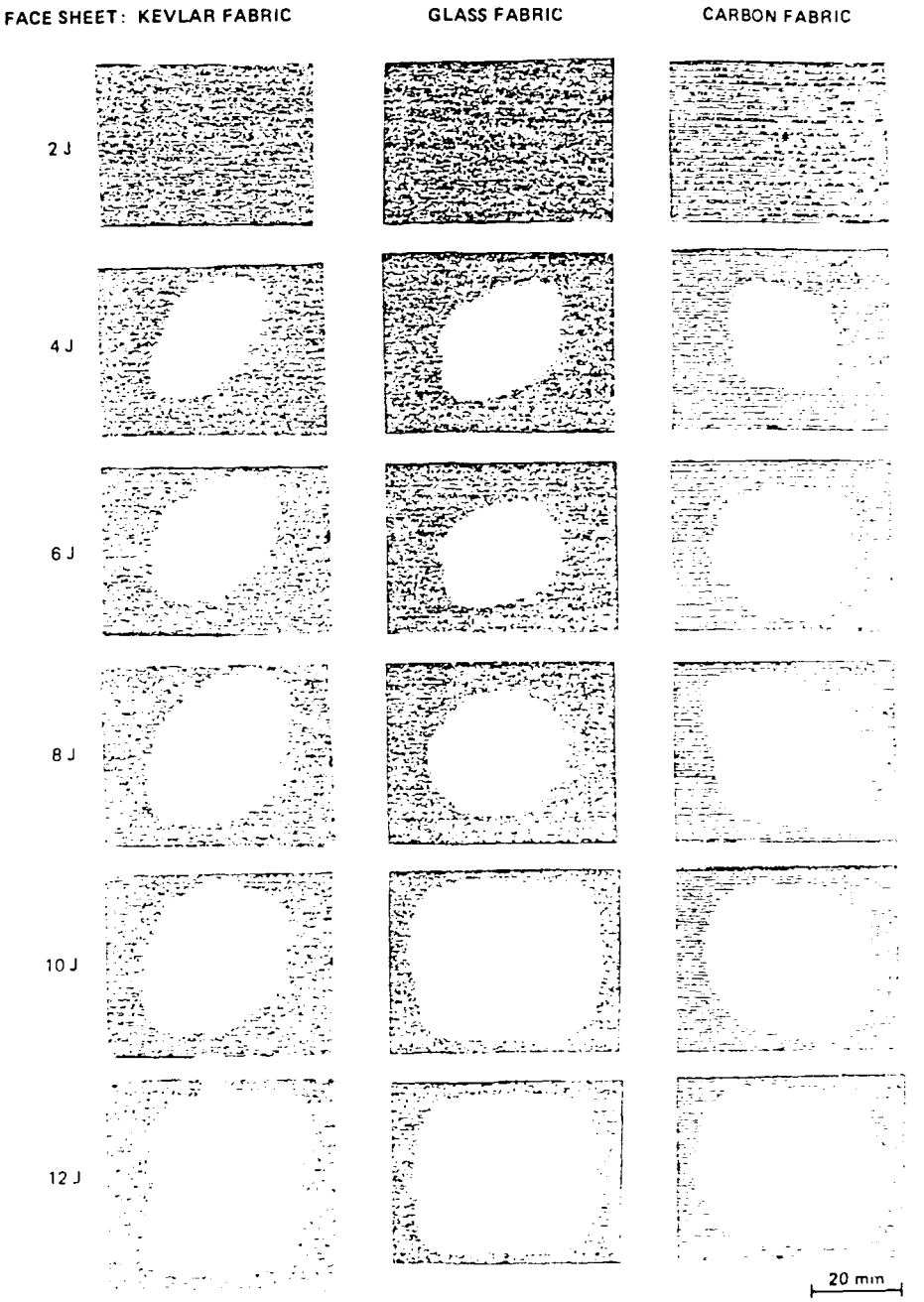

Fig 17 Ultrasonic C-scan images of impact tested laminates (NLR)

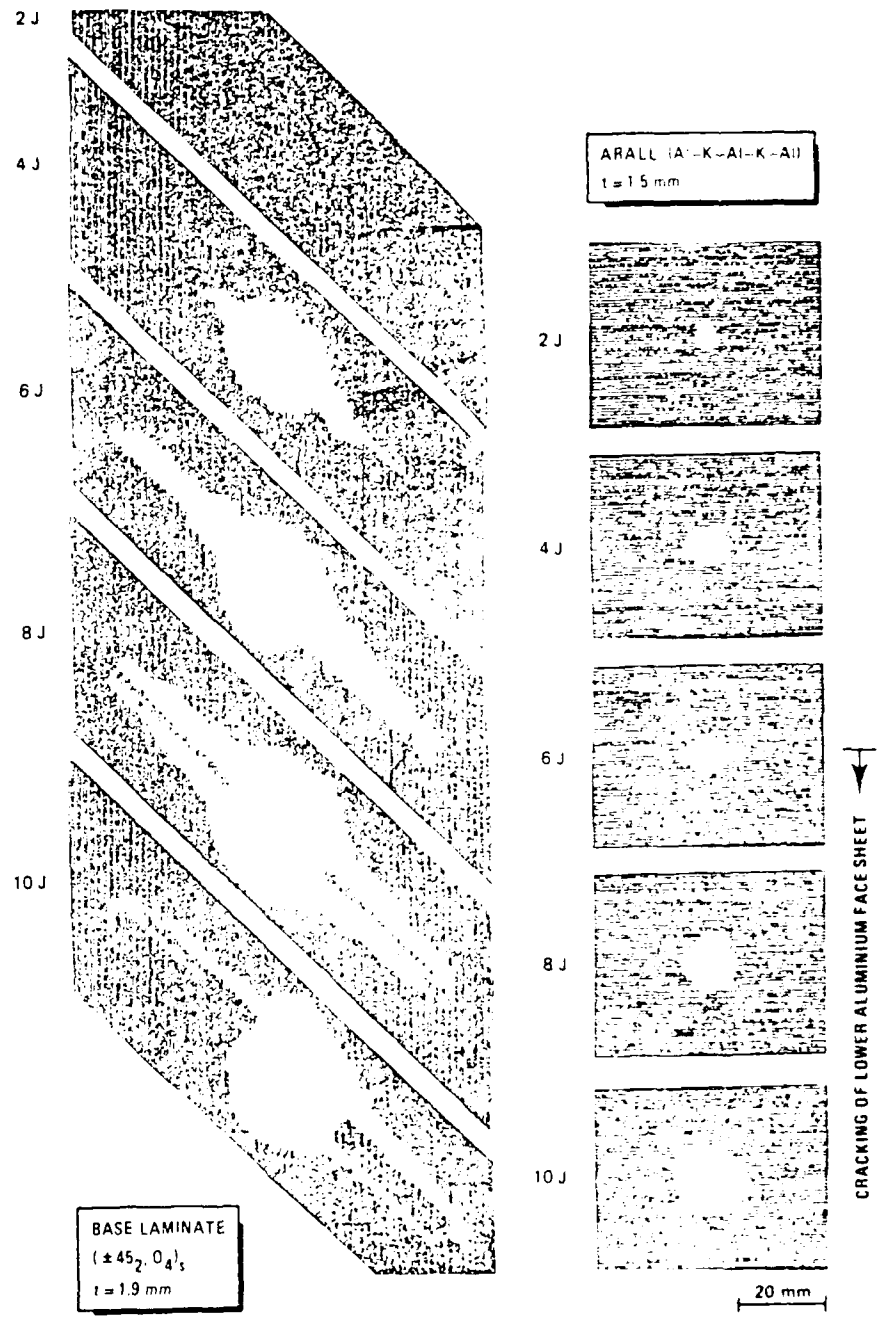

Fig 18 Ultrasonic C scan images of the impacted base laminate and ARALL (NLR)

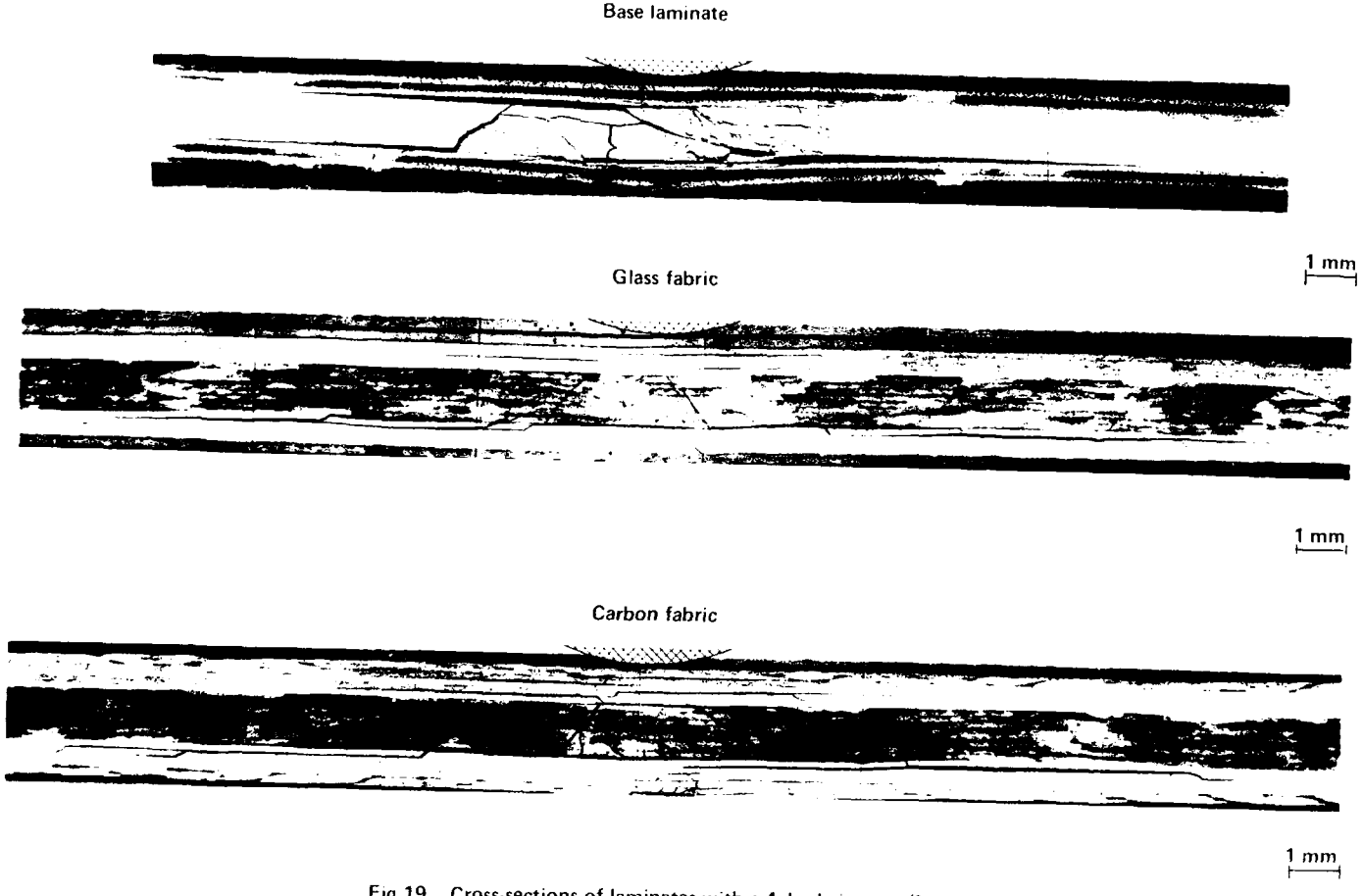

Fig 19 *Cross-sections of laminates with a 4 Joule impact (NLR)*

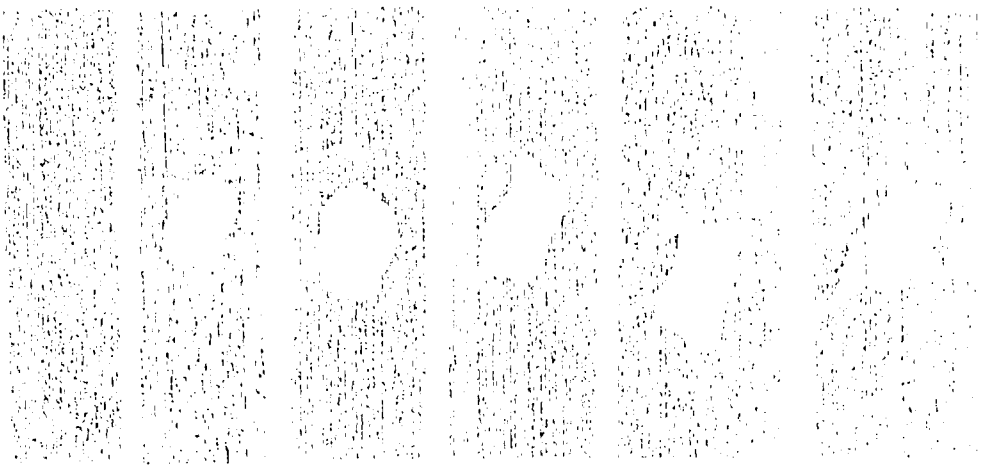

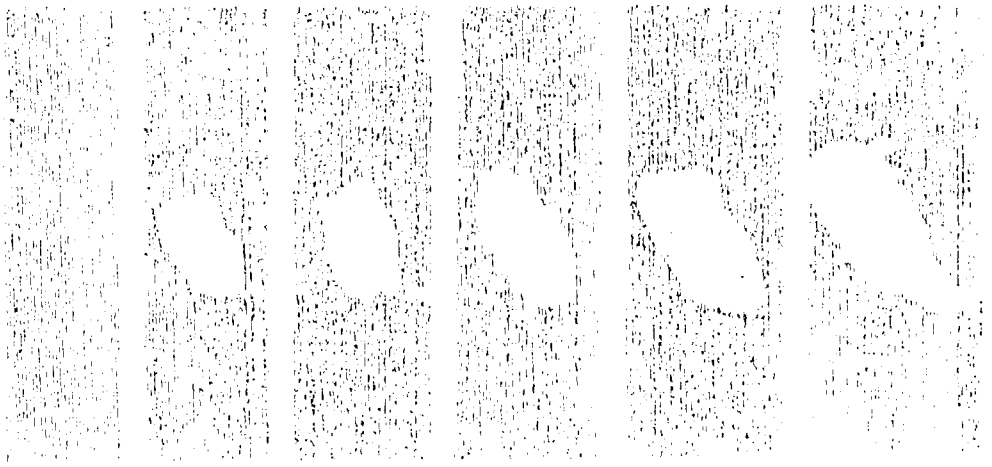

Fig 20 Ultrasonic C-scans of $[(\pm 45)_2, 0_4]_s$ carbon fibre laminates damaged by dropweight impact of various energies (ONERA)

Fig 21

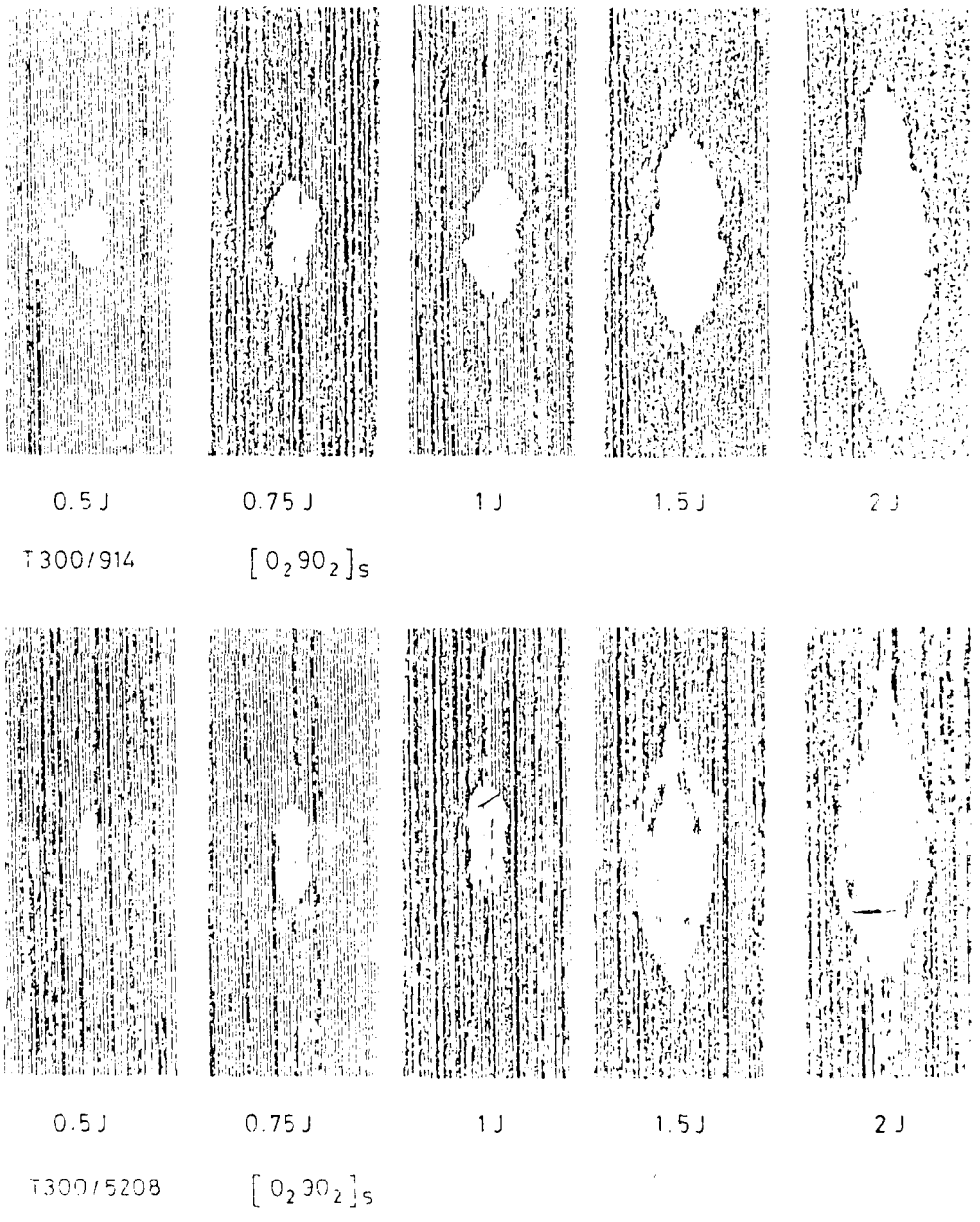

Fig 21 Ultrasonic C-scans of $[0_2, 90_2]_s$ carbon fibre laminates damaged by dropweight impact of various energies (ONERA)

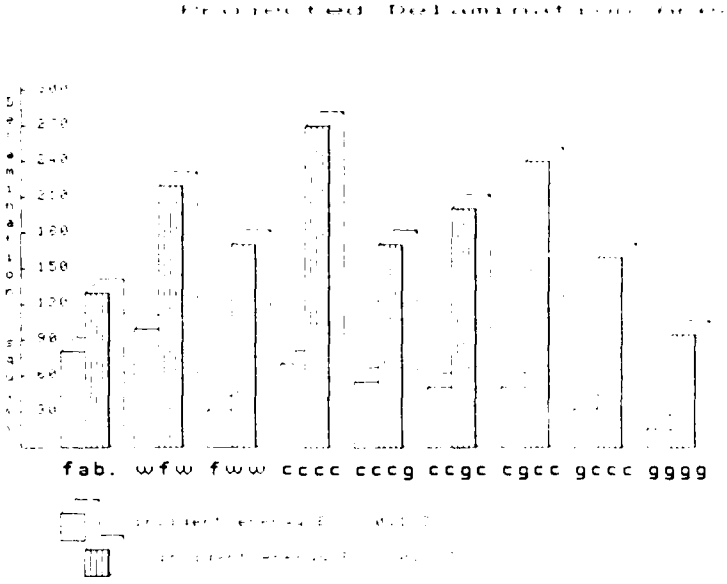

Fig 22 Delaminated areas caused by dropweight impact on various CFRP, GRP and CFRP/GRP hybrid laminates (DFVLR)

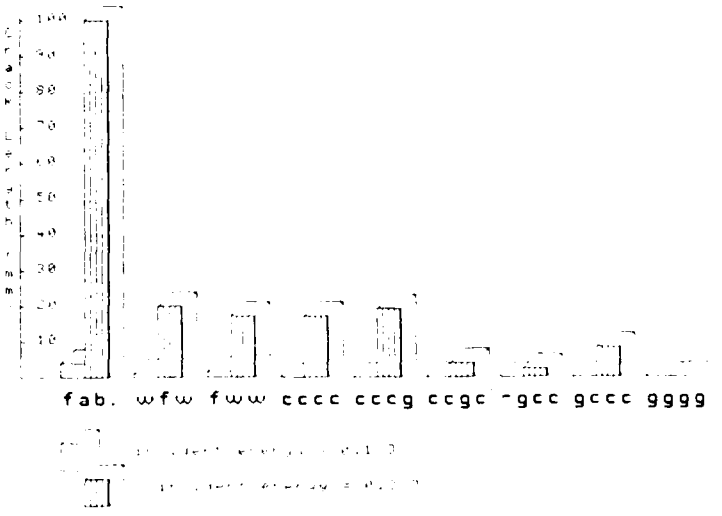

Fig 23 Amount of broken fibres caused by dropweight impact on various CFRP, GRP and CFRP/GRP hybrid laminates (DFVLR)

Fig 26

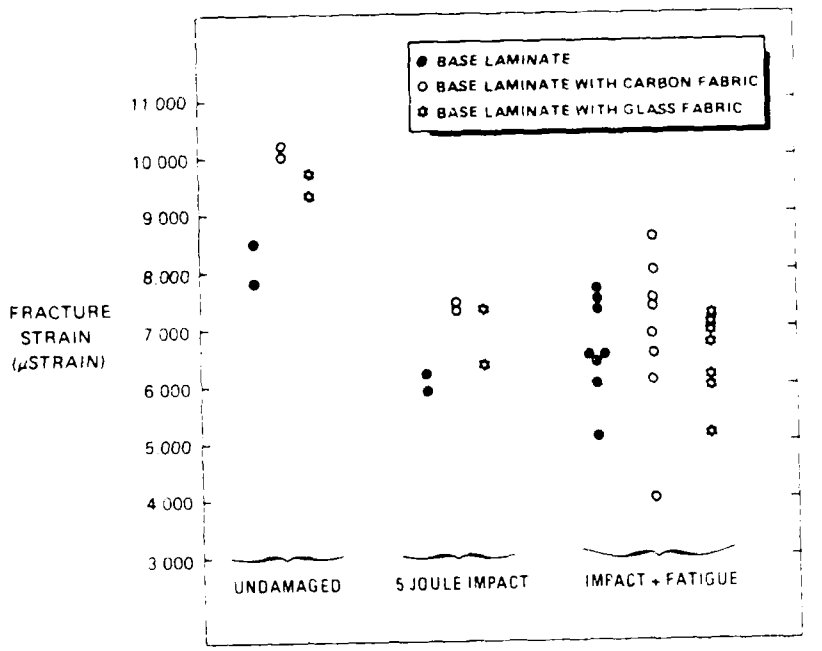

Fig 26 Compressive fracture strain of undamaged, impact damaged and fatigue tested laminates (NLR)

Fig 27

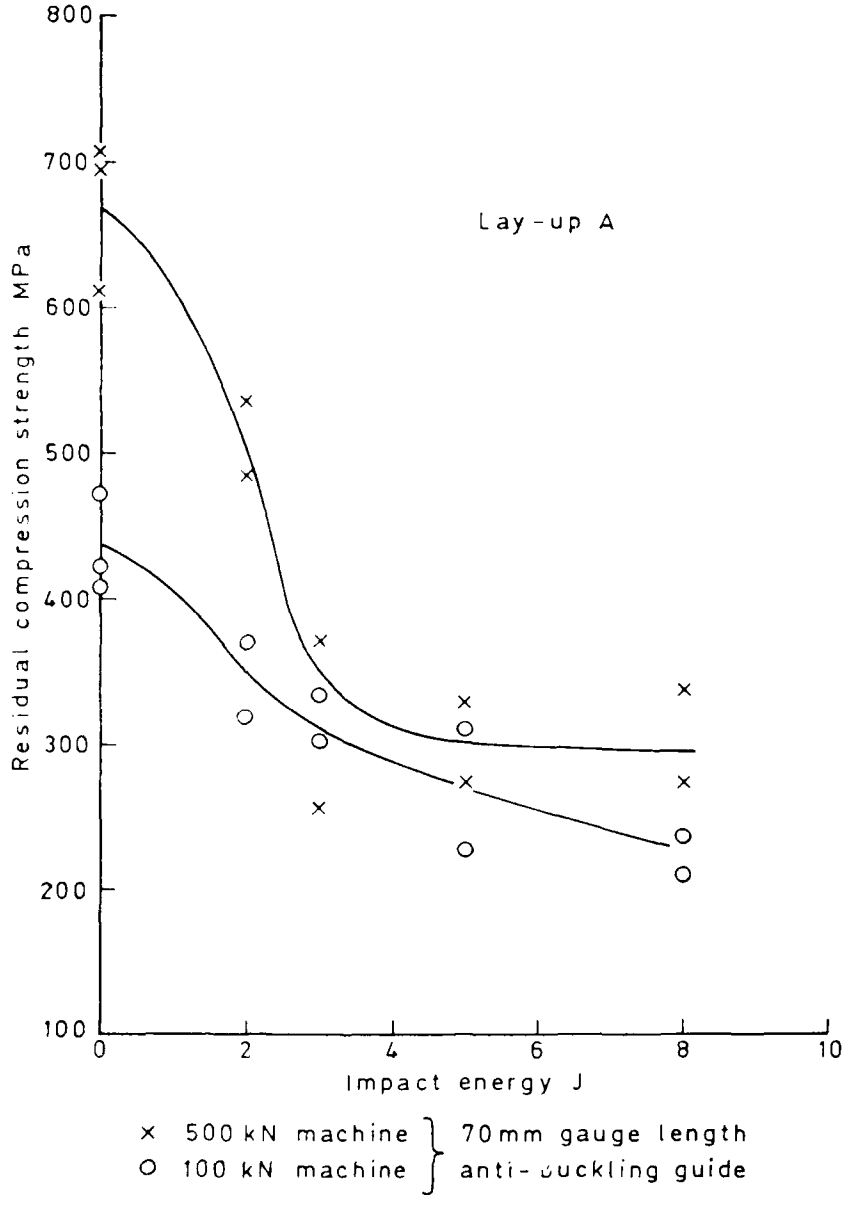

Fig 27 Effect of stabilising conditions on the residual compressive strengths of a carbon fibre laminate after impact (RAE)

Fig 28

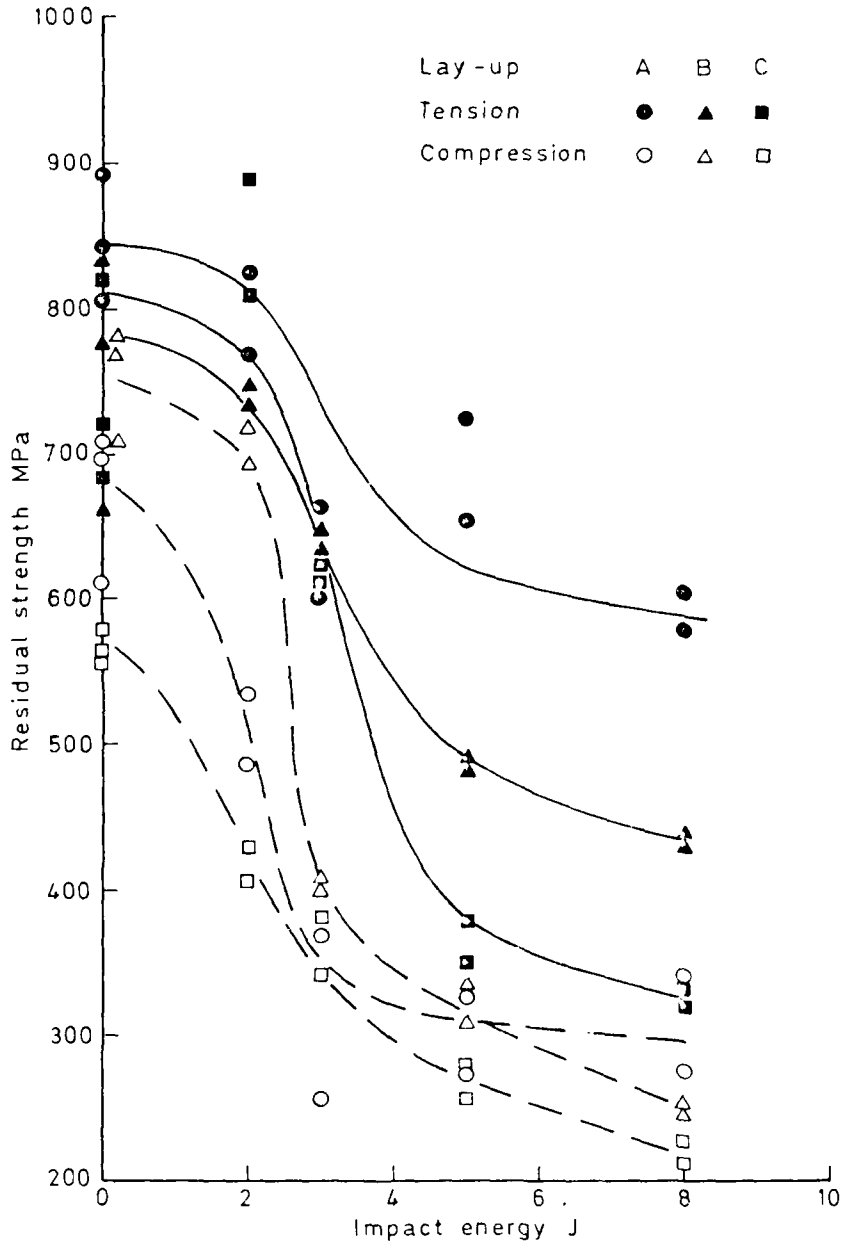

Fig 28 Effect of lay-up on the residual tensile and compressive strengths on 2mm thick carbon fibre laminates after impact (RAE)

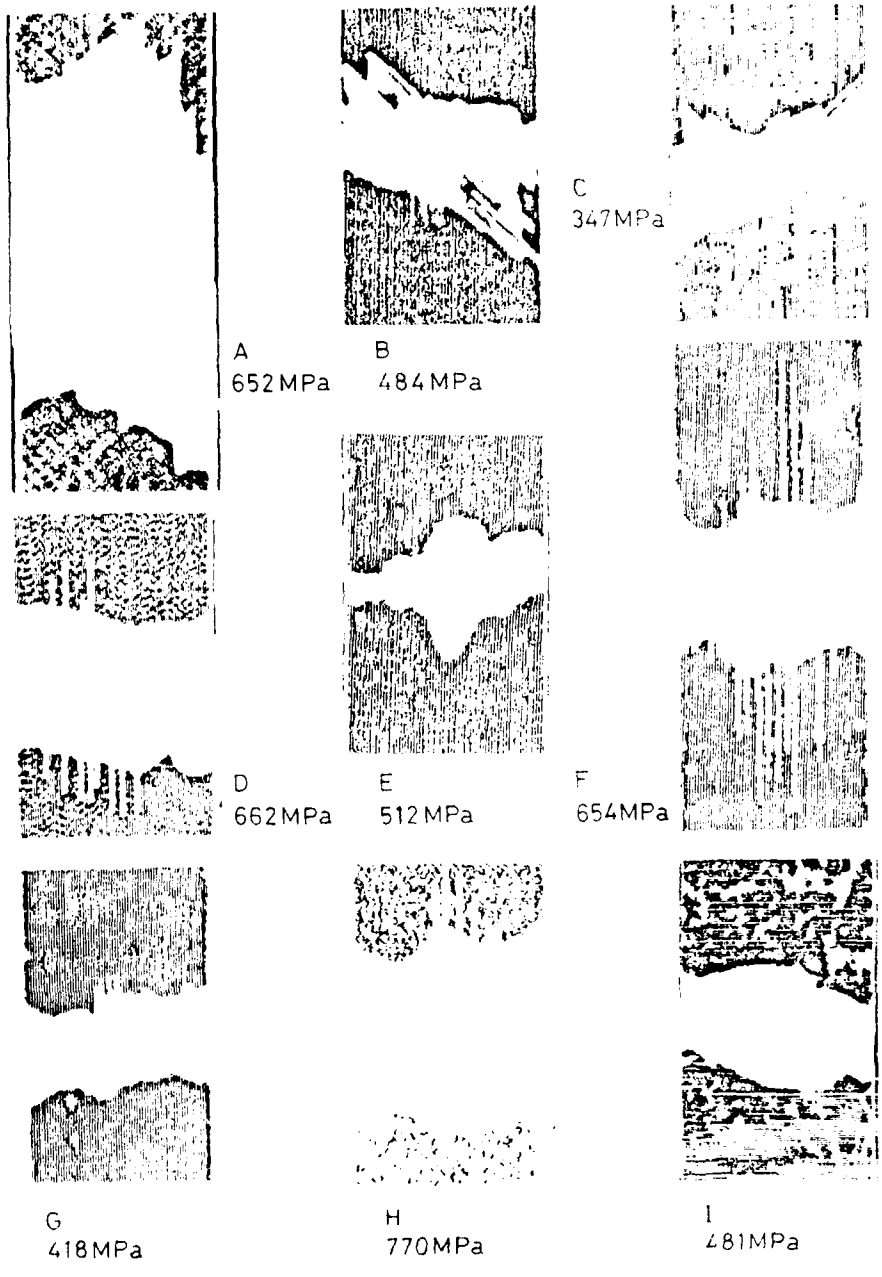

Fig 29 Ultrasonic C-scans of (0, ±45) carbon fibre laminates after 5J dropweight impact and tensile test to failure (RAE)

Fig 30

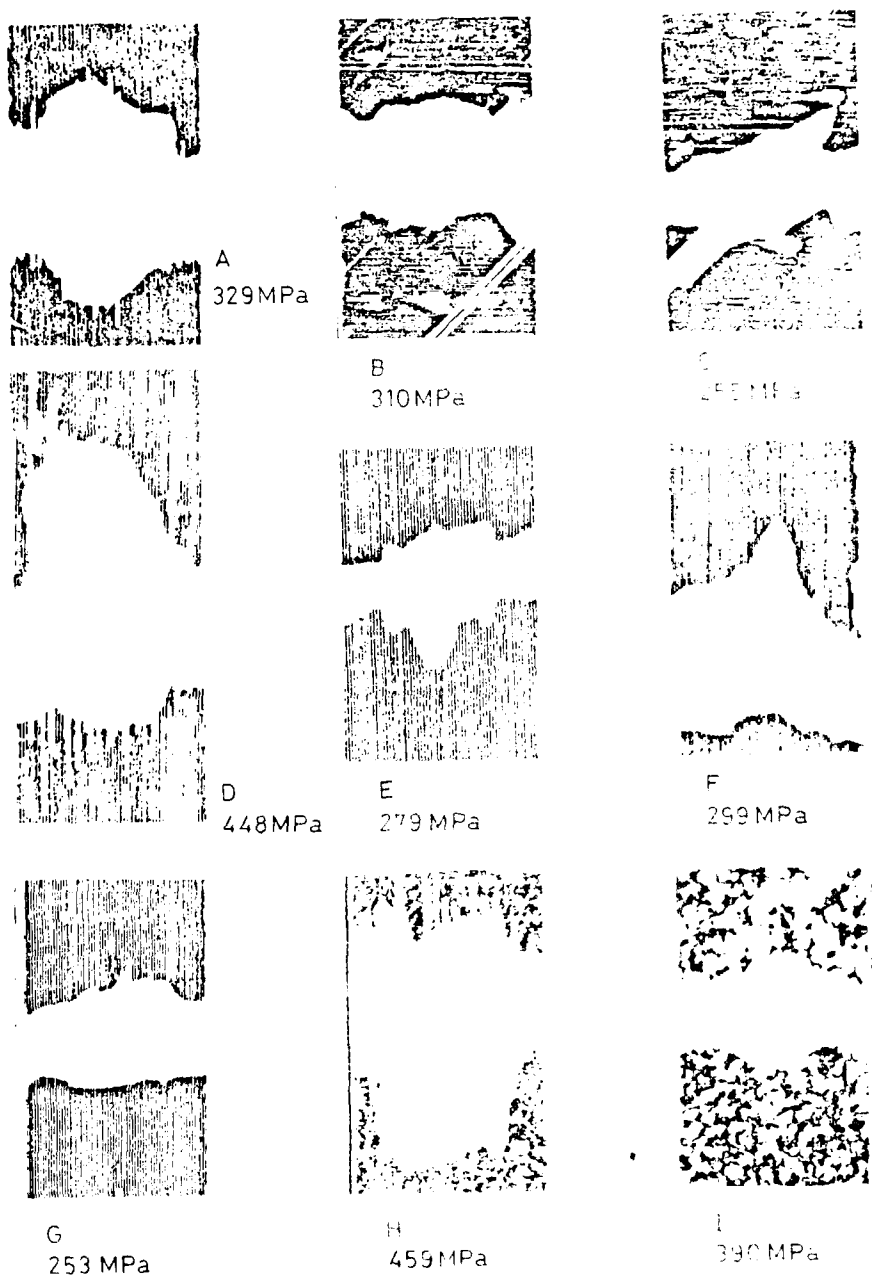

Fig 30 Ultrasonic C-scans of (0, ±45) carbon fibre laminates after 5J dropweight impact and compressive test to failure (RAE)

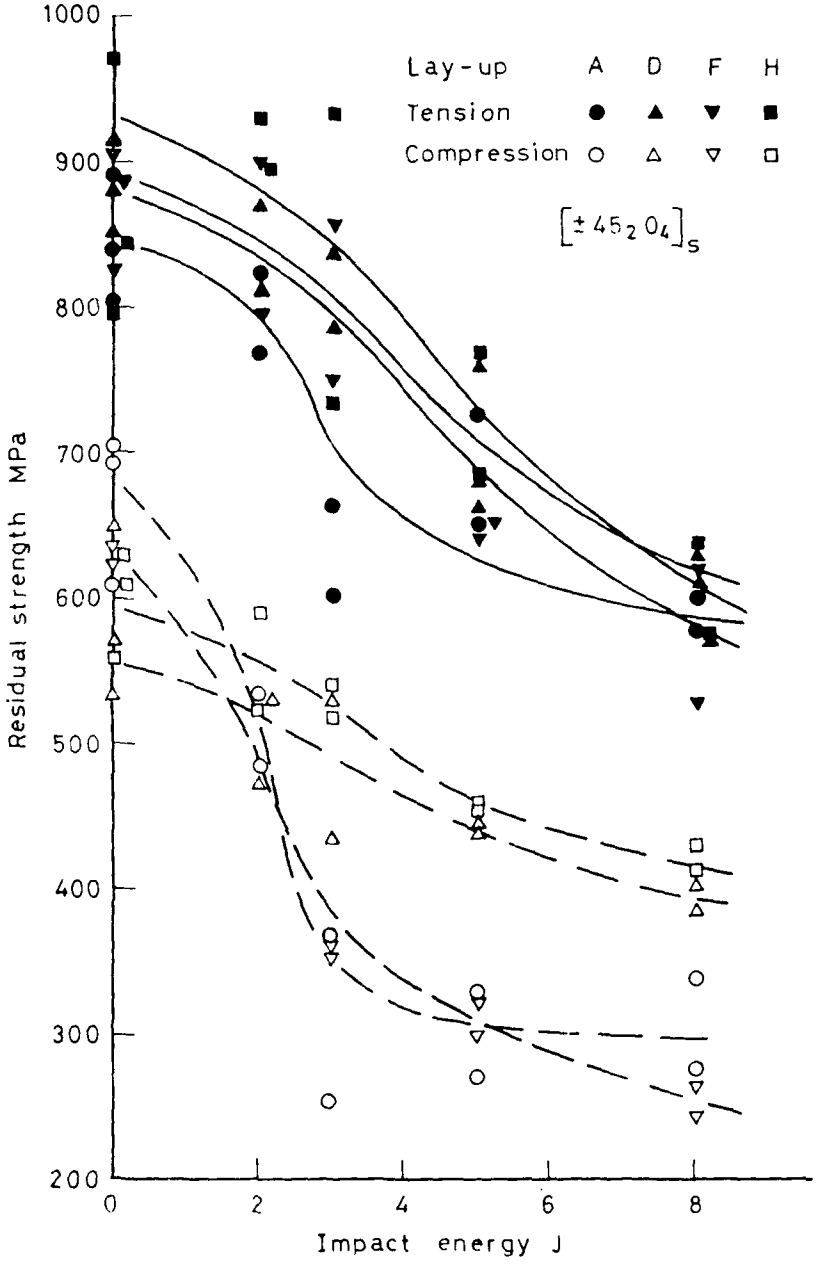

Fig 31 Effect of hybrid fabric plies on the residual strengths of 2mm thick carbon fibre laminates after impact (RAE)

Fig 32

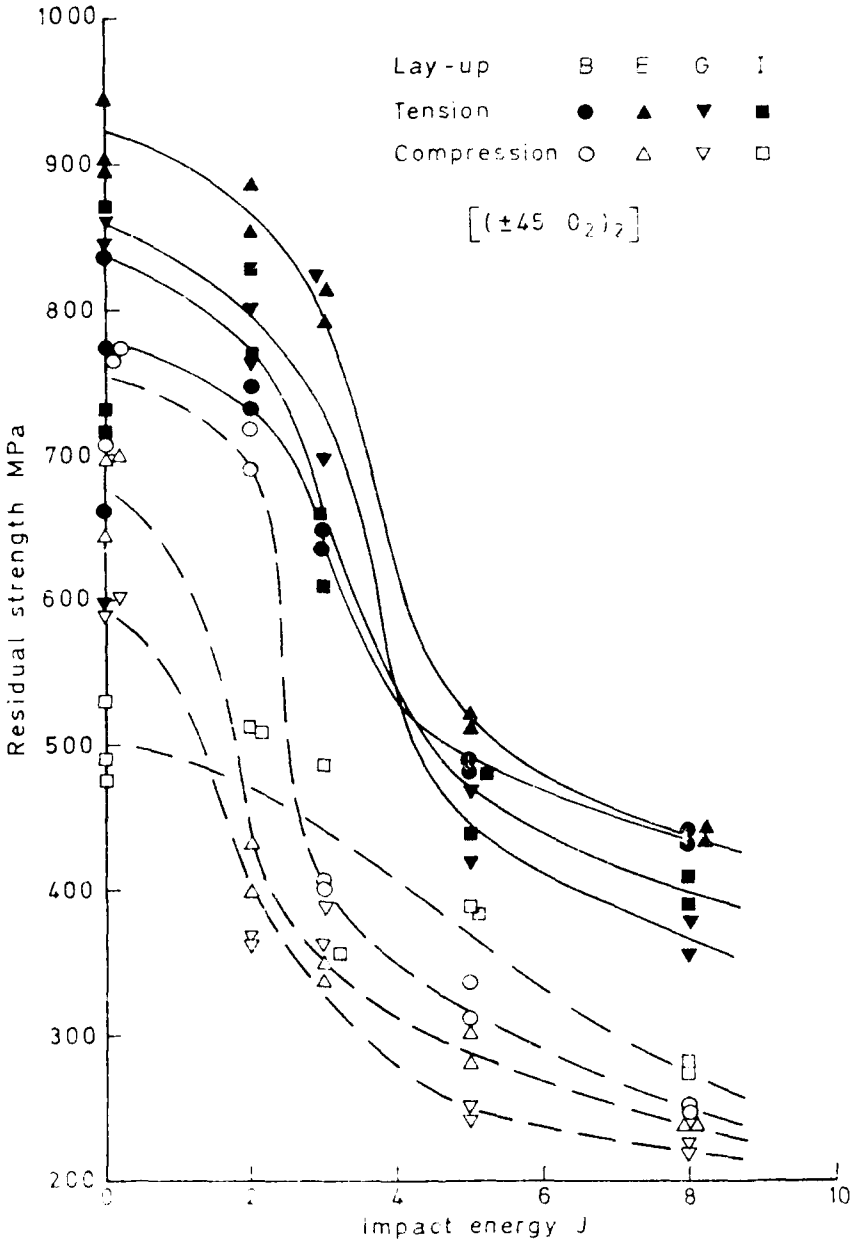

Fig 32 Effect of hybrid fabric plies on the residual strengths of 2mm thick carbon fibre laminates after impact (RAE)

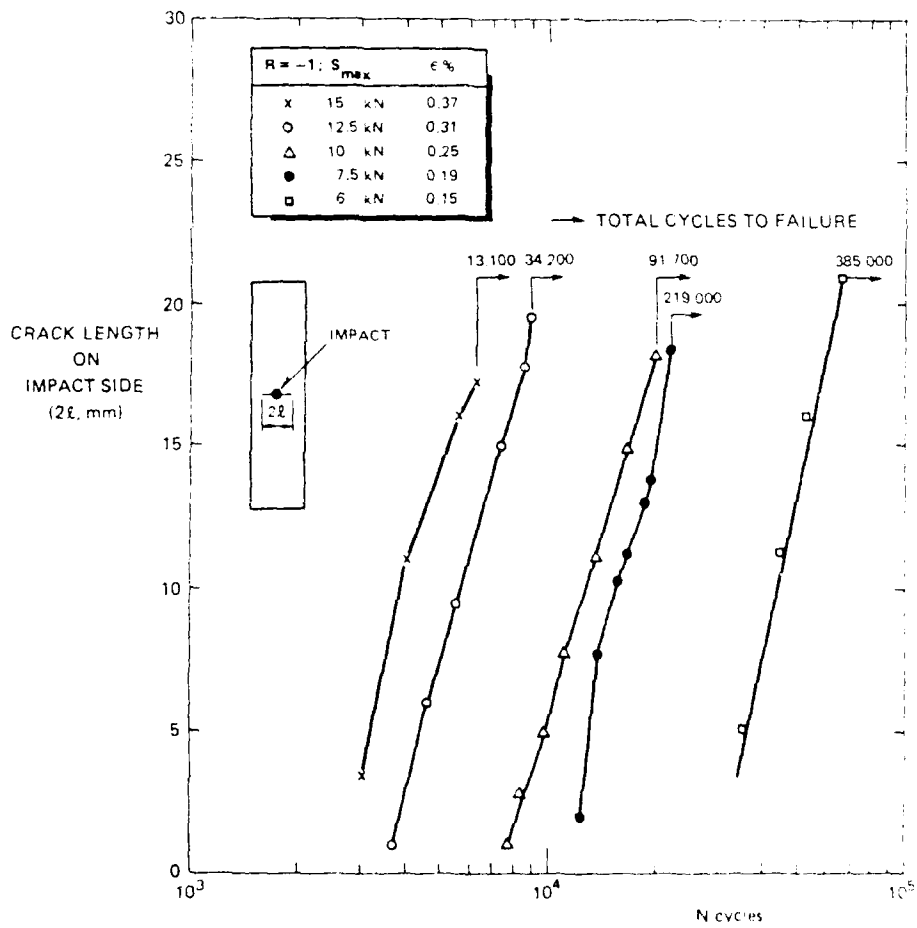

Fig 33 Crack propagation curves and fatigue lives of tested ARALL specimens (NLR)

Fig 34

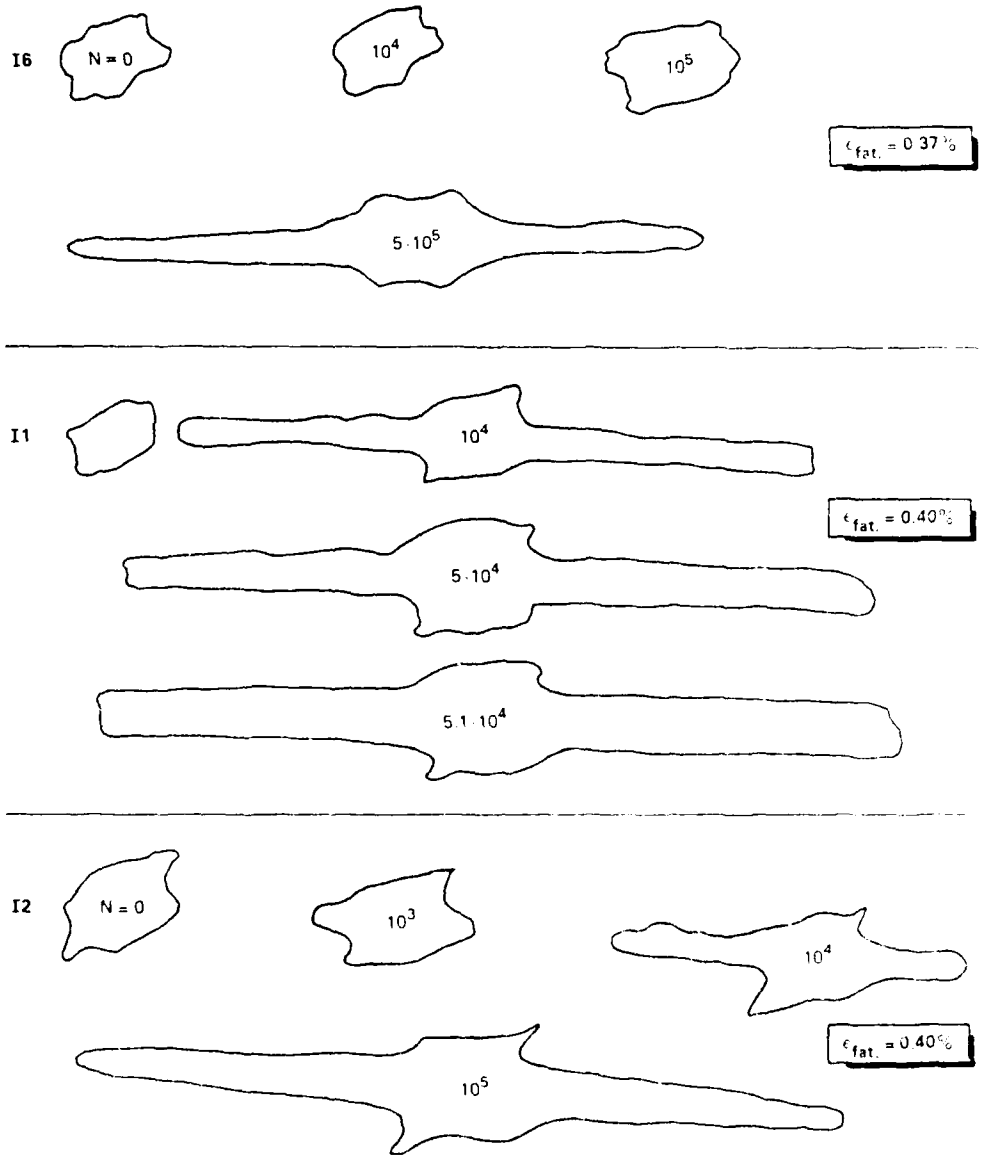

Fig 34 Ultrasonic C scan images of impacted coupon specimens after a specific number of fatigue cycles (base laminate) (NLR)

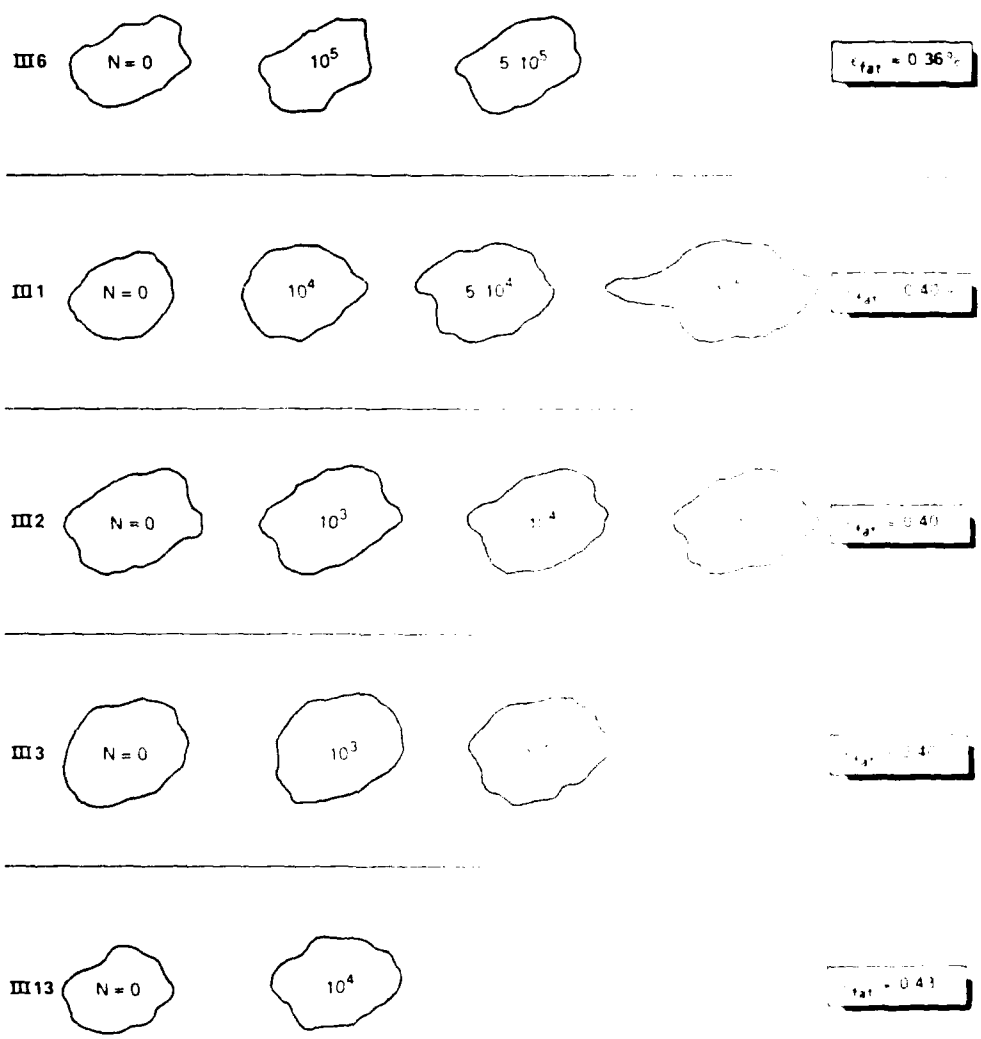

Fig 35 Ultrasonic C scan images of impacted coupon specimens after a specific number of fatigue cycles (base laminate with carbon fabric face sheets) (NLR)

Fig 36

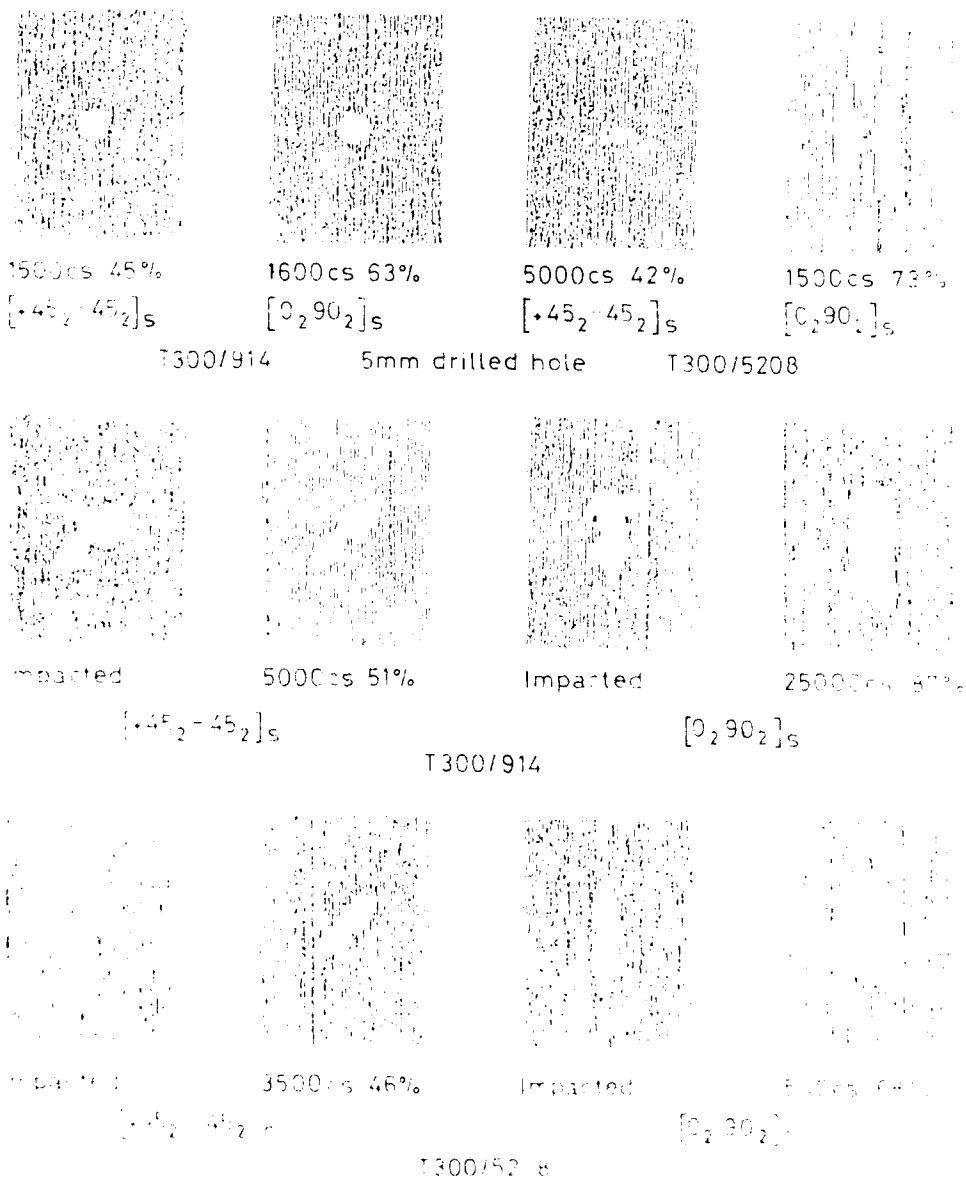

Fig 36 Ultrasonic C scans of damage growth in carbon fibre laminates produced by reversed axial fatigue for half the expected fatigue life (ONERA

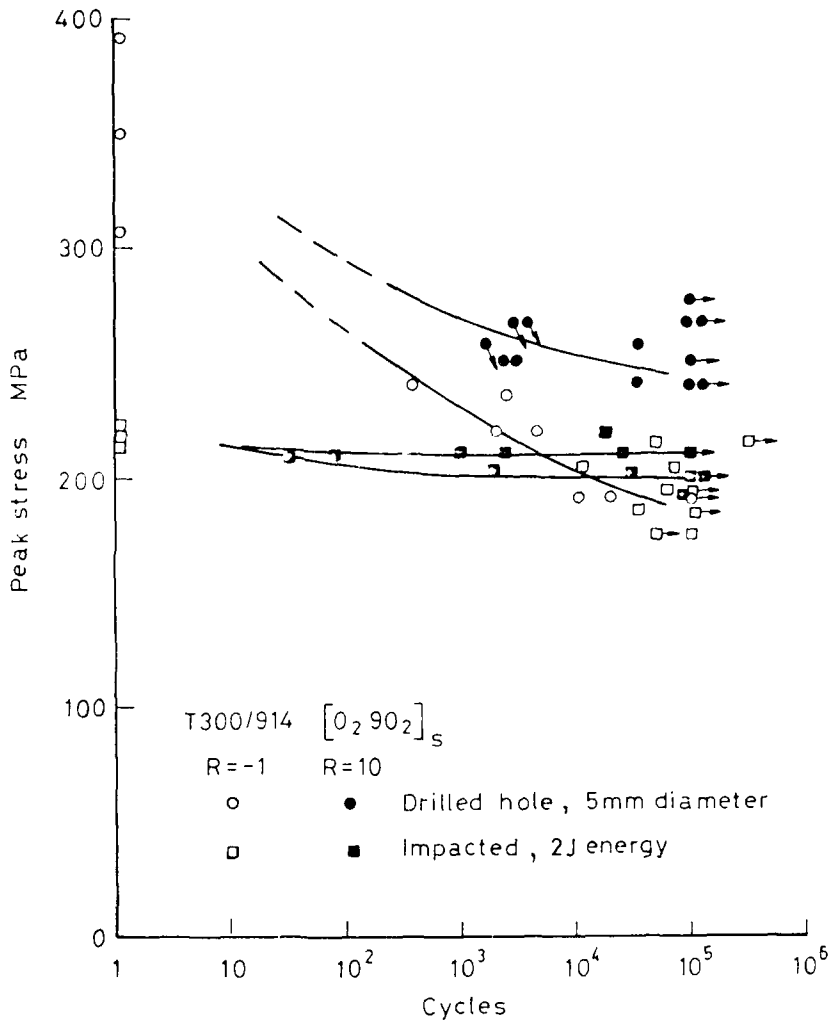

Fig 37 Reversed axial fatigue and axial compression fatigue of T300/914 $[0_2, 90_2]_s$ carbon fibre laminates with 5mm drilled hole or 2J impact energy (ONERA)

Fig 38

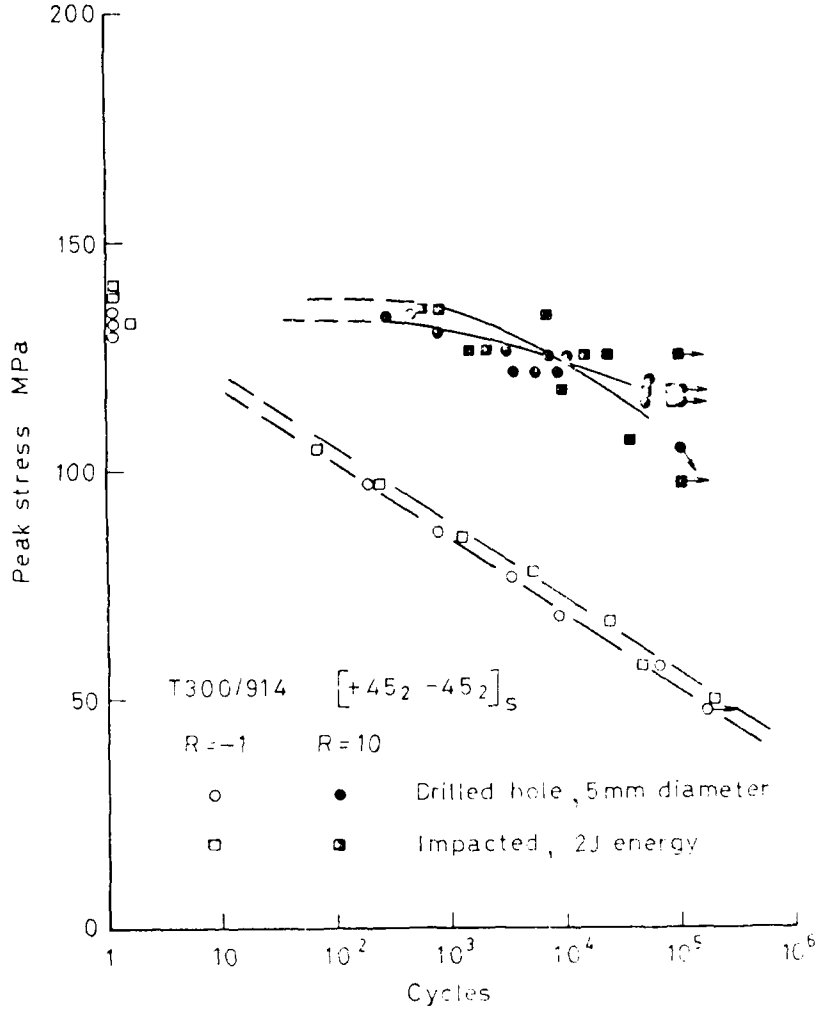

Fig 38 Reversed axial fatigue and axial compression fatigue of T300/914 $[+45_2, -45_2]_s$ carbon fibre laminates with 5mm drilled hole or 2J impact damage (ONERA)

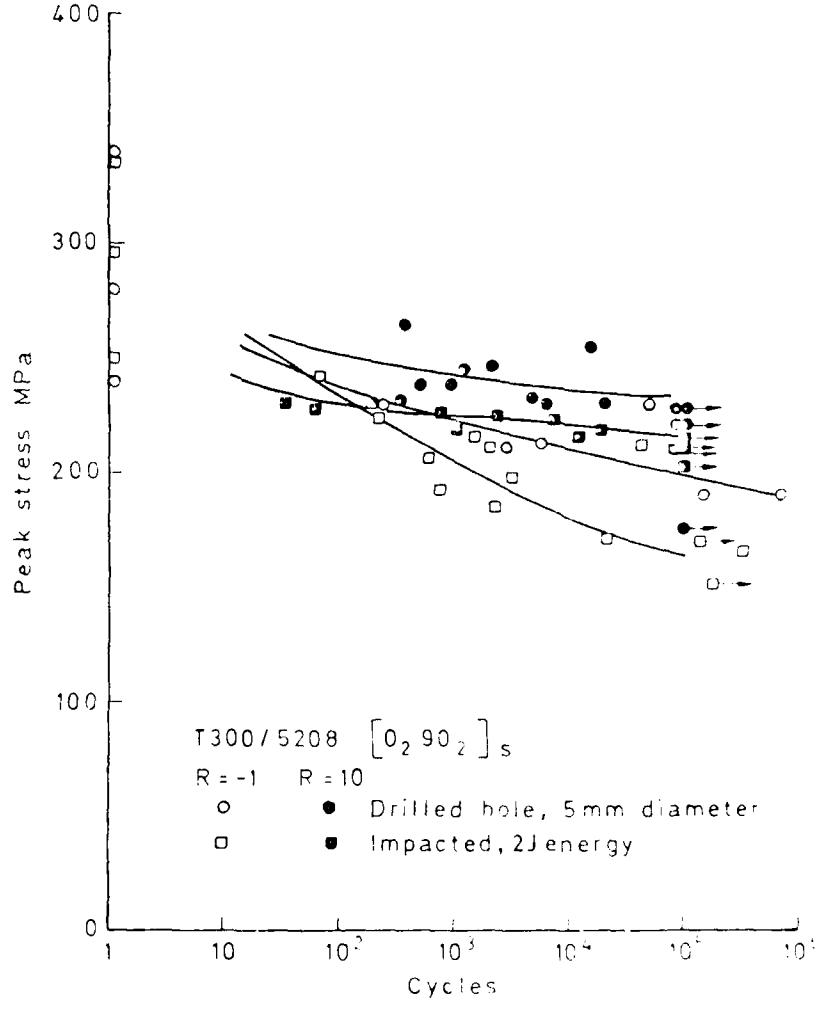

Fig 39 Reversed axial fatigue and axial compression fatigue of T300/5208 $[0_2, 90_2]_s$ carbon fibre laminates with 5mm drilled hole or 2J impact damage (ONERA)

Fig 40

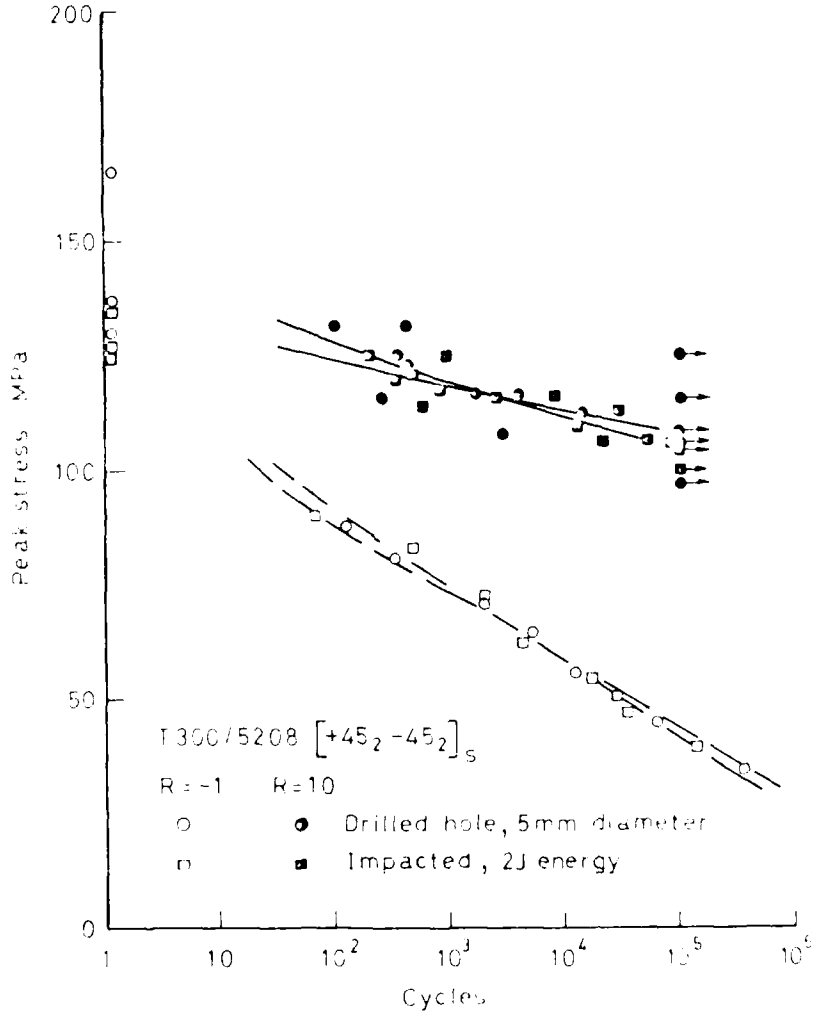

Fig 40 Reversed axial fatigue and axial compression fatigue of T300/5208 $[+45_2, -45_2]_s$ carbon fibre laminates with 5mm drilled hole or 2J impact damage (ONERA)

Fig 41

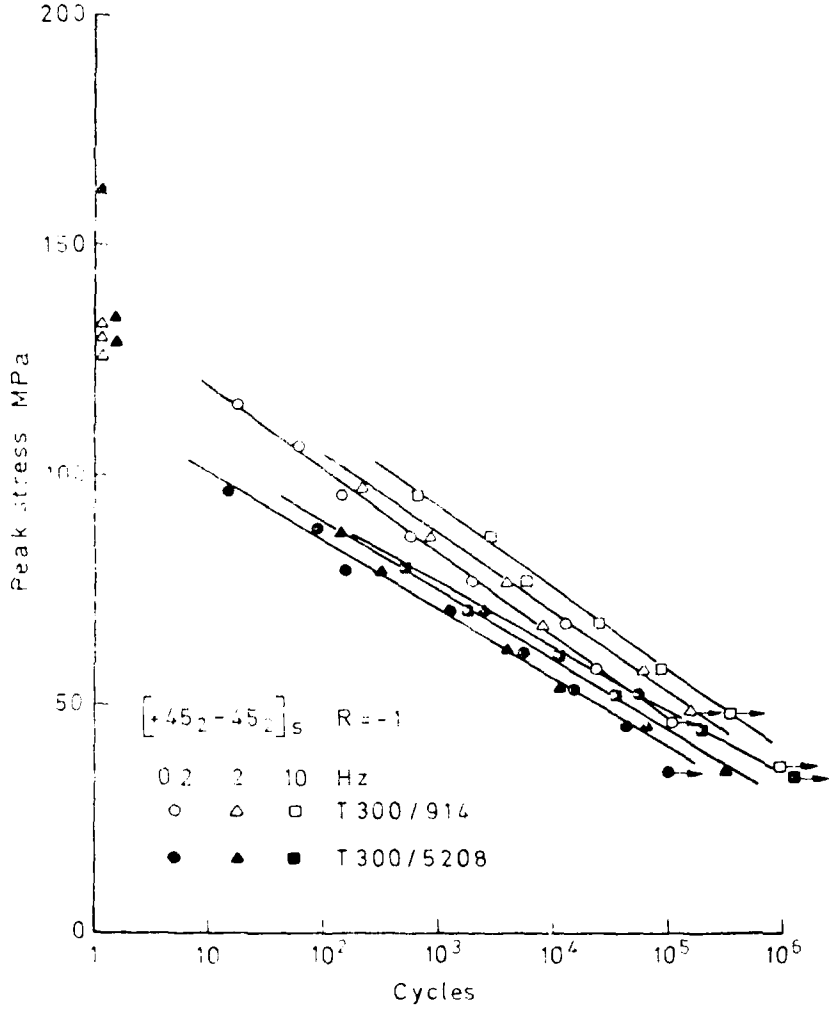

Fig 41 Effect of test frequency on the reversed axial fatigue of $[+45_2, -45_2]_s$ carbon fibre laminates with 5mm drilled hole (ONERA)

Fig 42

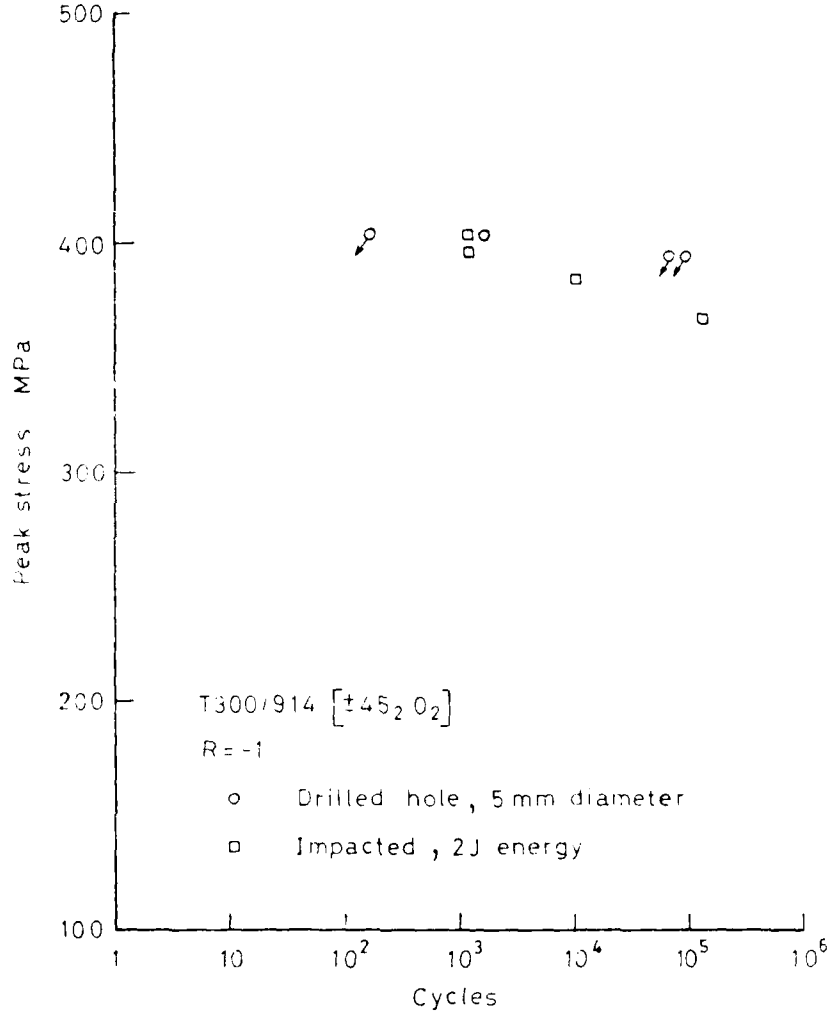

Fig 42 Reversed axial fatigue of T300/914 $[(\pm 45)_2, 0_4]_s$ carbon fibre laminates with 5mm drilled hole or 2J impact damage (ONERA)

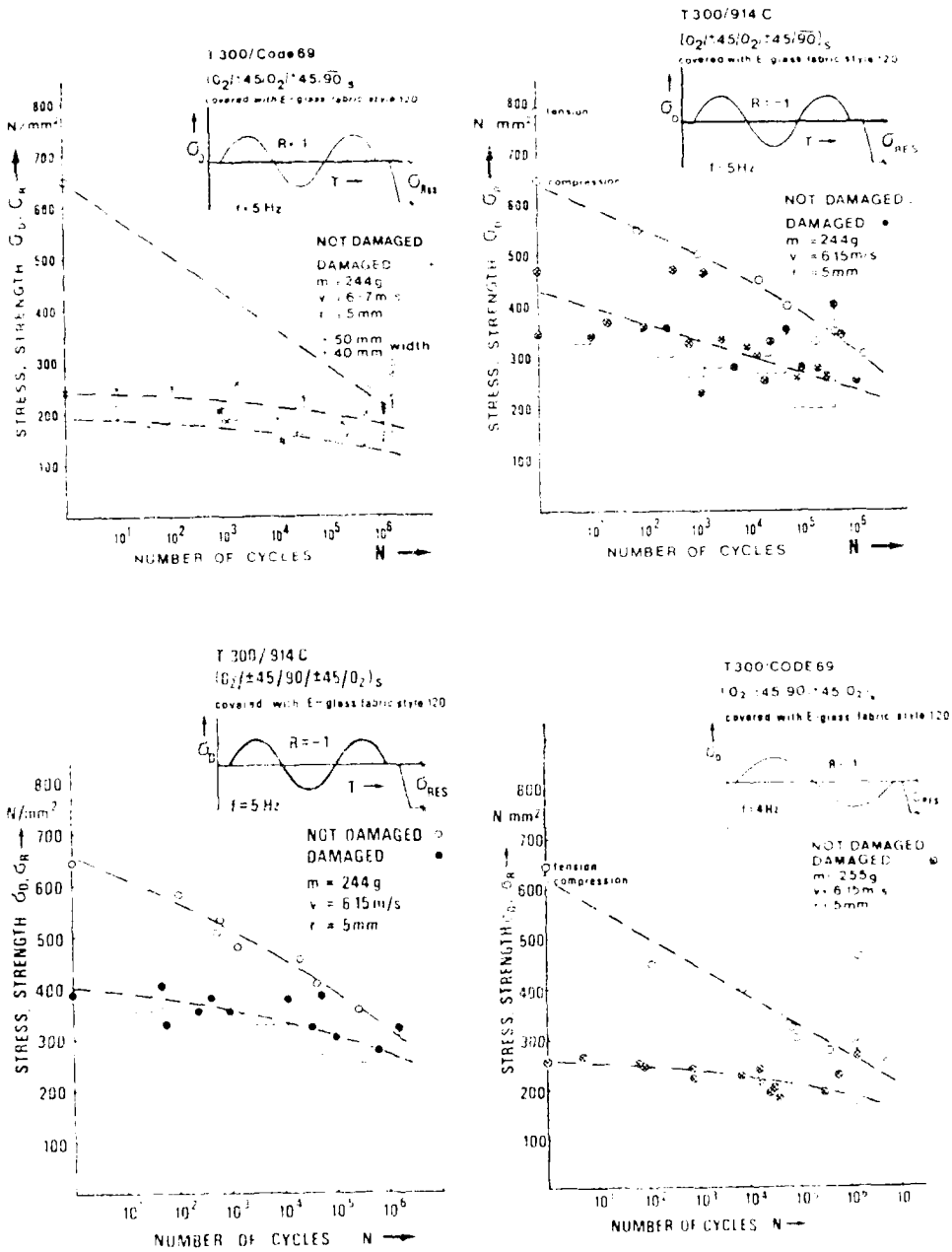

Fig 43 Fatigue curves (R = -1) for undamaged and impact damaged carbon fibre laminates (DFVLR)

Fig 44

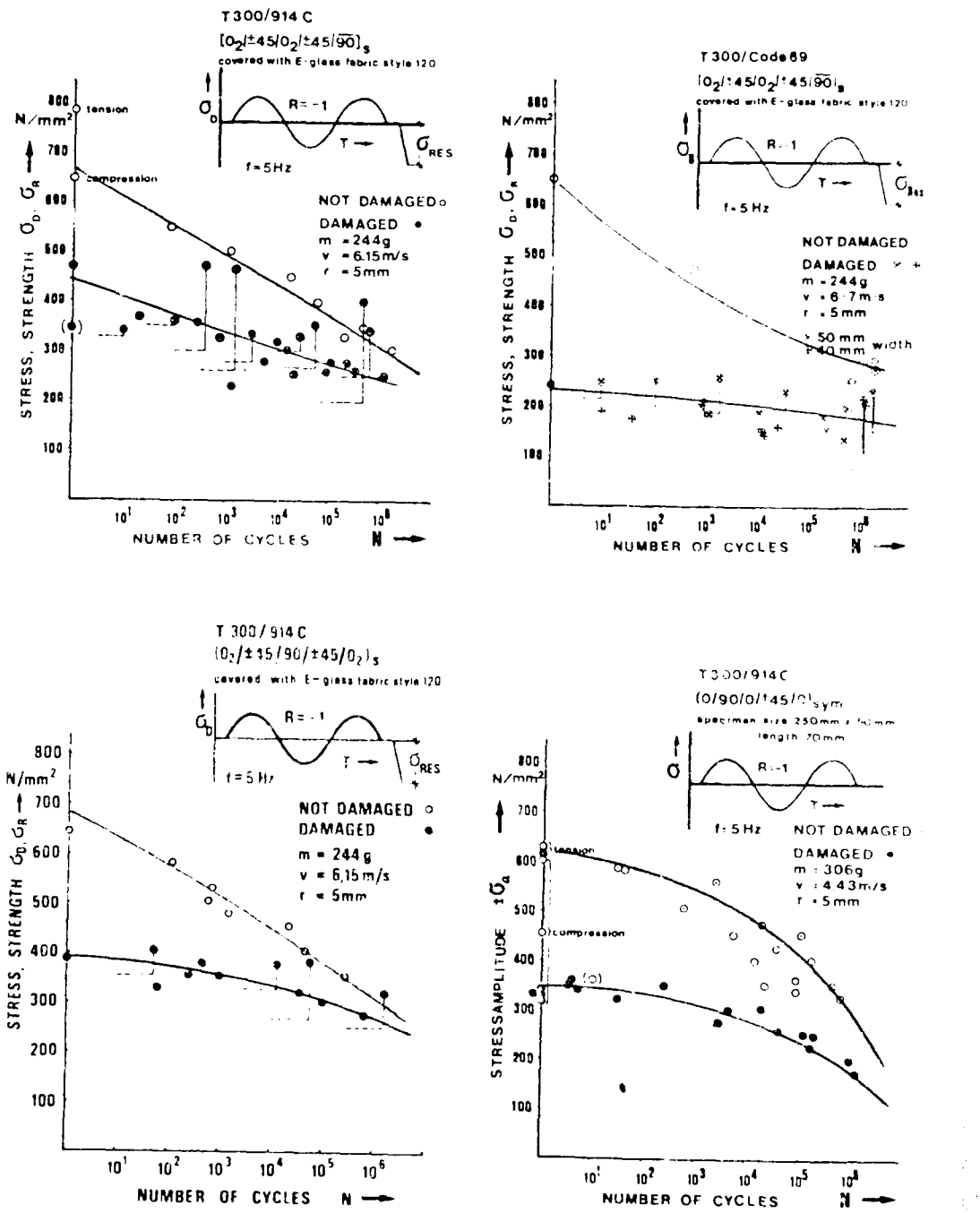

Fig 44 Fatigue curves (R = 1) for undamaged and impact damaged carbon fibre laminates (DFVLR)

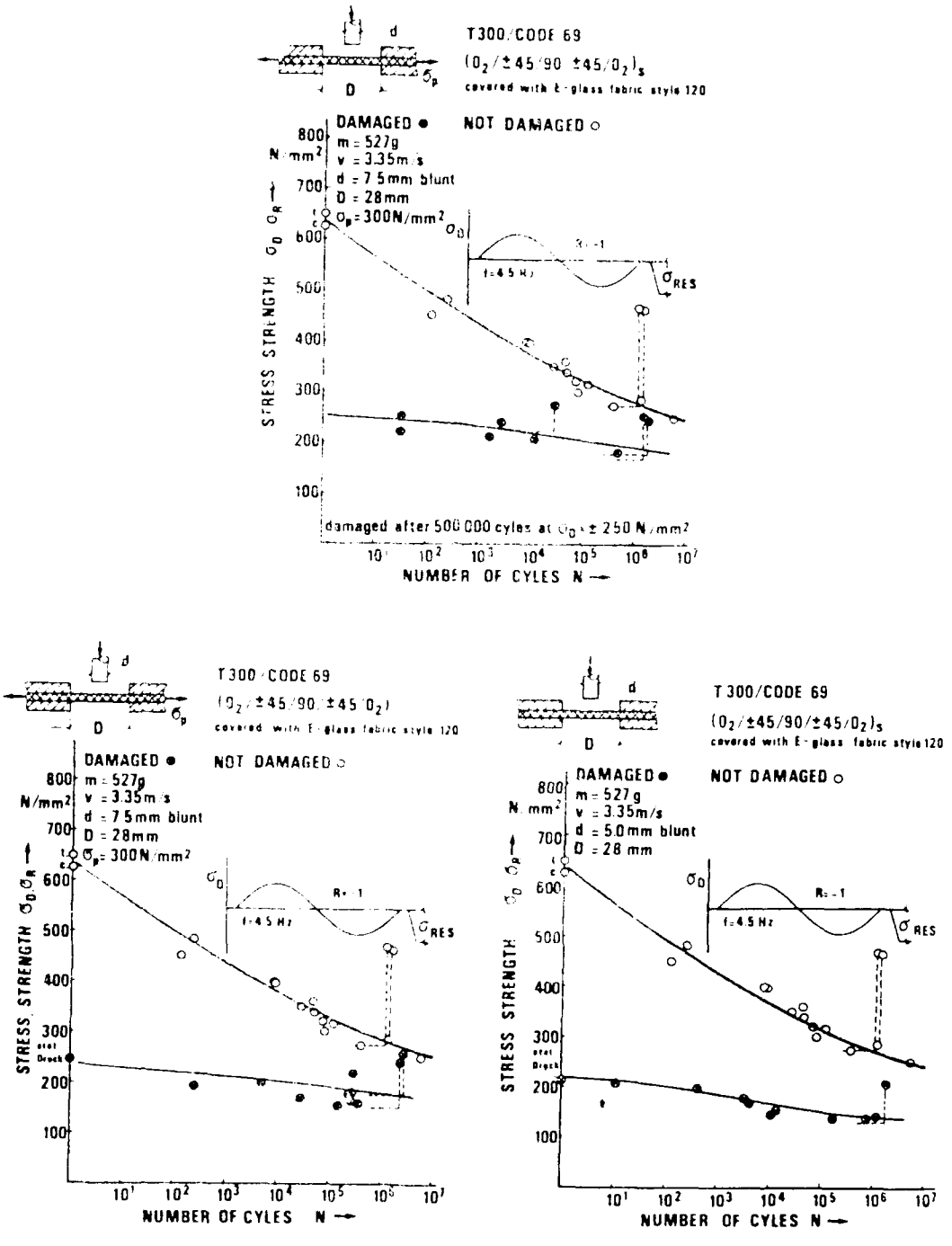

Fig 45 Fatigue curves (R = -1) for undamaged and impact damaged carbon fibre laminates (DFVLR)

. ig 16

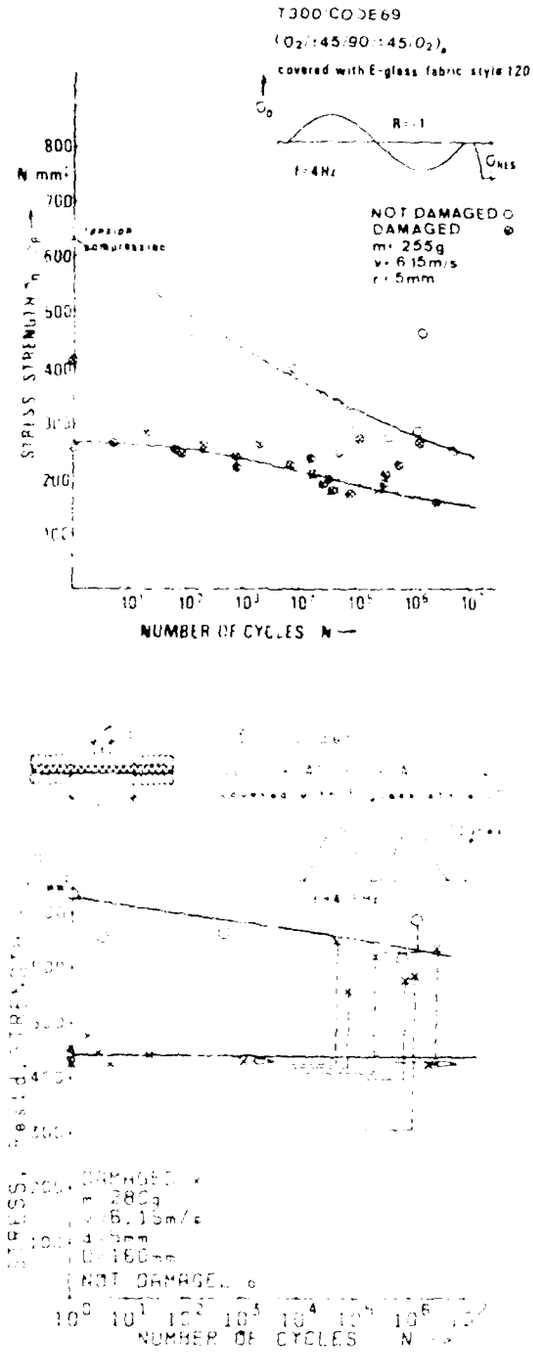

Fig 46 Fatigue curves (R = 1, R = 0) for undamaged and impact damaged carbon fibre laminates (DFVLR)

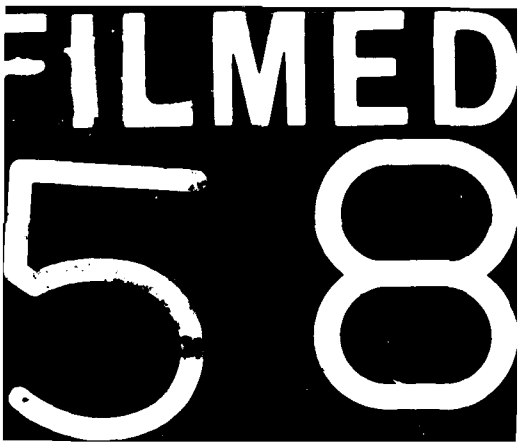
FILMED
58